ON CYCLODEXTRIN INCLUSION COMPLEXES AS SHIFT REAGENTS IN TRAVELING-WAVE ION MOBILITY SPECTROMETRY

A Thesis
Presented to
The Academic Faculty

by

Ken Laszlo

In Partial Fulfillment
of the Requirements for the Degree
B.S. Chemistry in the
School of Chemistry and Biochemistry

Georgia Institute of Technology
May 2012

ON CYCLODEXTRIN INCLUSION COMPLEXES AS SHIFT REAGENTS IN TRAVELING-WAVE ION MOBILITY SPECTROMETRY

Approved by:

Dr. Facundo Fernández, Advisor
School of Chemistry and Biochemistry
Georgia Institute of Technology

Dr. Andrew Lyon
School of Chemistry and Biochemistry
Georgia Institute of Technology

Dr. William Baron
School of Chemistry and Biochemistry
Georgia Institute of Technology

Date Approved: April 27, 2012

ACKNOWLEDGEMENTS

I wish to thank Dr. Facundo Fernández for his mentorship and guidance in writing this document, as well as his support over the last two years in acquiring this data. In addition, I would like to thank my mother and father for their support and generosity over the last two decades.

TABLE OF CONTENTS

LIST OF FIGURES

LIST OF TABLES

LIST OF SYMBOLS AND ABBREVIATIONS

MS	Mass Spectrometry
IMS	Ion Mobility Spectrometry
IM-MS	Ion Mobility Mass Spectrometry
T-Wave	Travelling Wave Ion Mobility Spectrometry
NMR	Nuclear Magnetic Resonance
CID	Collision Induced Dissociation
CCS	Collision Cross Section
Ω	Collision Cross Section
m/z	Mass to Charge Ratio
Å	Angstrom (10^{-10} meters)
SA	Sphinganine
SO	Sphingosine
CD	Cyclodextrin
PC	Phosphatidylcholine
PMG	1-palmitoyl-2-myristoyl-*sn*-glycero-3-phosphocholine
Leu-Enk	Leucine-enkephalin
α-, β-, γCD	Alpha, beta, and gamma-cyclodextrin
Amino-βCD	3A-Amino-3A-deoxy-(2AS,3AS)-beta-cyclodextrin
HP-βCD	2-Hydroxypropyl-beta-cyclodextrin
NPC	Niemann-Pick Disease Type C
NPC1	Niemann-Pick Gene 1
NPC2	Niemann-Pick Gene 2

SUMMARY

Detection of lipids and lipid/cyclodextrin complexes is a nontrivial aspect in novel treatments of Niemann-Pick disease type C. Recently, the FDA approved Hydroxypropyl-β-cyclodextrin as a treatment for the condition, as it had shown promising results in mice in the removal of neurodegeneration biomarkers.[1] Several lipids of concern in Niemann-Pick disease type C, and their corresponding cyclodextrin complexes were detected via traveling-wave ion mobility mass spectrometry (T-Wave-MS). In addition to detection alone by MS, collision cross sections (CCS) of the ions were measured within the T-Wave cell, to give insight as to the size of the complexes. As shown, using cyclodextrins to complex lipids shifts their place within the m/z vs. CCS space, aiding the spectral interpretation process for detecting the complexes.

Additionally, a study of how wave height within the T-Wave cell effects the CCSs obtained was performed. Here, evidence for dipole alignment within the T-Wave cell is presented, as ions of greater rigidity show smaller CCSs at greater wave heights.

CHAPTER 1

INTRODUCTION

Recently, the FDA approved Hydroxypropyl-Beta-Cyclodextrin as a treatment for Niemann-Picks Disease Type C (NPC).[1a] NPC is a relatively rare genetic disorder involving the NPC1 and NPC2 gene that affects 1:150,000 people of western European ancestry.[2] Of the two genes, mutations in the NPC2 gene account for only about 4% of cases; previously this was given the title "Niemann-Picks disease type D," however it is now recognized as the same condition.[2] The disease affects lipid storage in the body, specifically the intracellular movement of lipids, like glycosphingolipids, and cholesterol.[1b, 2] This results in several fatal conditions such as ascites, ataxia, and respiratory failure.[2] Onset may occur at any age, and can result in developmental issues in infants and children.[2] Due to this newfound use as a treatment for NPC, cyclodextrin molecules have become particularly significant to the pharmaceutical industry.[1a, 3]

Cyclodextrin molecules are cyclic compounds composed of 6-8 glucopyranoside monomers bound in a conical fashion (named alpha- beta-, and gamma-cyclodextrin respectively). The monomers' unique orientation produces a hydrophilic outer shell and a hydrophobic inner shell, whose inner radius is 0.57 nm, 0.78 nm, and 0.95 nm for alpha-, beta-, and gamma-cyclodextrin, respectively.[4] Hydrophobic moieties (CH_2-, etc.) comprise the interior of the structures, while the outside holds the hydrophilic functional groups of the glucose monomers (-OH). This structure allows cyclodextrin rings the unique ability to act as a "host" to "guest" hydrophobic molecules by forming non-

covalent inclusion complexes; this in turn increases the solubility of hydrophobic molecules in aqueous solution.[3]

The formation of guest-host complexes in solution have significant implications in treating lipid-related diseases and drug delivery.[1a, 5] Cyclodextrin guest-host complexes have been identified with several classes of molecules, including aromatics, barbiturates, and dicarboxylic acids in both negative and positive ion mode mass spectrometry (MS).[6] Several tools, such as UV-visible spectroscopy, NMR, and mass spectrometry can used to determine the orientation and stoichiometry for such complexes.[6b, 7] As, noted by Tabushi et al. the guest-host complexes are mostly driven by van der Waal interactions, however the conformational energy of cyclodextrin, and the collapse of water clusters are important thermodynamic factors as well.[8] Still, cyclodextrin-lipid complexes have not yet been studied in detail, despite their emerging use as new drugs for treating lipid storage metabolic disorders.

This project aims to determine the collision cross sections (CCS) of several cyclodextrin molecules, and cyclodextrin-lipid complexes via traveling wave ion mobility (T-wave) measurements. CCS values represent the conformational structures of molecules in the gas phase; however these measurements are dependent on the gas used to collide with the molecule of interest. E.W. McDaniel at Georgia Institute of Technology invented ion mobility spectrometry in the 1950's and 60's.[9] Since then several variants of the original technique have been employed and commercialized, including the traveling-wave ion mobility spectrometer (T-Wave).

T-wave is a relatively new form of ion mobility spectrometry (IMS), which has become popular in the MS community due to its commercial availability in the Waters

Synapt G2 HDMS system.[9b, 10] The instrument functions by pulsing an electric potential wave in the same direction as an ion beam passing through a "drift region." In opposition to the ion beam is a low pressure inert gas (usually Helium or Nitrogen on the order of 1-5 torr), called a "drift gas".[10b] Collisions with the drift gas will slow ions, and therefore the ions will have a longer drift time through the T-Wave cell. Thus, ions are separated by their CCSs, as ions with larger CCSs will have more collisions with the drift gas.

Guest-host interactions, similar to those shown here, have proven beneficial in ion mobility spectrometric (IMS) separations.[11] Because guest-host complexes have a different CCS value than the naked guest, the host shifts the drift time of the guest in the IMS dimension. Therefore, these guest-host interactions can aid in separating molecules of interest from a potentially complex matrix. Additionally, guests can be removed from their hosts via collisional-induced dissociation (CID) to do the weak van der Waals forces holding the complex together.[11] This allows for separation of guest-host complexes from complex solutions, followed by detection of the naked guest by MS/MS.

The main advantage IMS has over other separation techniques is its ability to rapidly separate molecules of different sizes. Where chromatographic techniques may require a tens of minutes to a an hour for a complete separation, IMS separations occur in milliseconds. In addition, it has been shown that coupling IMS separations prior to mass analysis increases the peak capacity of an experiment.[11a, 12] IM-MS separations employing a shift reagent have recently been shown to increase peak capacity to approximately 2400; nearly twice the reported peak capacity of IM-MS experiments performed without a shift reagent.[11c]

Despite the high-throughput capabilities of IMS, the technique does have a few drawbacks. T-wave, in particular suffers from low resolution (due to the drift cell being at a reduced pressure), and mobility-dependent resolution; drift tube ion mobility spectrometry, however does have much improved resolution compared to T-Wave.[10b] In addition to T-wave's low resolution the separation is not completely orthogonal to mass analysis, by which it is usually accompanied.[11c] The ion's flight down the drift tube is determined by two related factors: its CCS value and its mass to charge ratio (m/z). Thus, IM-MS analysis does not exploit the m/z vs. CCS space to its full extent. Still, as we demonstrate here, IMS is a powerful, convenient, and fast technique for separating gas-phase ions prior to mass analysis.

In the early stages of development of T-wave separations, there was a lack of a standard procedure for calibrating the T-wave drift times to obtain CCS values due to a lack of theoretical understanding of how the separation inside the drift cell occurred; nevertheless, work leading to a new calibration method was published in 2004.[13] Since then, more advanced theory and calibration methodologies for T-wave IMS have been developed.[10b, 14] The calibration method Ruotolo published in 2008 is employed in this work.[14a] This calibration external standard, which is then used to construct a calibration curve, allowing for drift times obtained experimentally to be used to calculate CCS values.

To date, T-wave has been shown to give accurate and precise CCS values of biologically relevant species that match those from previously established techniques like x-ray crystallography and NMR within 2% error.[10a] In addition, studies have shown that gas-phase proteins retain their aqueous-phase densities within the ion mobility drift tube;

this is significant because it shows that conclusions drawn about molecular structures from ion mobility studies not only match other techniques, but also reflect solution conformations within biological systems.[14b]

The work presented here demonstrates fundamental aspects of T-wave-MS and its application of biological systems. First, T-wave was used to reveal the structural diversity of ESI-formed clusters of various cyclodextrins and calculate their CCS values. Several cyclodextrin-lipid complexes were also studied in this manner. Additionally, the effect of the traveling wave electric field magnitude (wave height) on the calculated CCS value was determined. This study provides new insights on the complexation of lipids in cyclodextrin-containing solutions, as well as the limits of the analytical instruments used to examine them.

CHAPTER 2

MATERIALS AND METHODS

All lipids used were purchased from Avanti Polar Lipids (Alabaster, Alabama). Lipids were stored at -80˚C prior to being opened. Once opened, lipids were dissolved in 1:1:1 MeOH:H_2O:AcN and refrigerated. Cyclodextrins were purchased from TCI America (Portland, OR) and stored at room temperature. Cholesterol and Polyalanine were purchased from Sigma Aldrich (St. Louis, MO). Solvents used were purchased from EMD. All materials were used without further purification.

Solutions of cyclodextrin molecules, cyclodextrin-lipid complexes, and polyalanine were dissolved in a solution of 50/50 (v/v) methanol/water. Cholesterol was dissolved in 2:1 methanol/chloroform (v/v), and experiments containing both cholesterol and HP-βCD were also dissolved in 2:1 methanol/chloroform (v/v). For T-wave calibration, a solution of polyalanine was used at a concentration of approximately 33 nM.

For T-wave-MS experiments, a Waters SYNAPT G2 ion mobility mass spectrometer was used. The instrument is equipped with an electrospray ionization source (ESI) held at 4.0 kV for positive mode and -2.8 kV for negative mode with a sample solution flow rate of 25 μL/min. Following ionization, the ions are guided to a quadrupole mass filter, and into the T-wave. After IMS separation, the ions are pushed into an orthogonal acceleration time-of-flight mass analyzer equipped with a reflectron (*oa*-reToF). The instrument specifics are further outlined elsewhere.[15] The T-wave drift cell was set to a wave height of 30 V and velocity of 300 m/s unless otherwise noted.

Nitrogen was used as the drift gas throughout the experiments. Nitrogen was purchased from Airgas (Atlanta, GA). The pressure within the T-wave was held at 3.7 Torr.

CHAPTER 3

CCS CALCULATIONS

The calibration method employed here was first outlined by Ruotolo, as mentioned earlier.[14a] Briefly, CCS values are traditionally determined via drift-tube IMS experiments using the Mason-Schamp equation:

$$\Omega = \frac{18\pi^{\frac{1}{2}}}{16}\frac{ze}{k_B T^{\frac{1}{2}}}\left[\frac{1}{m_I}+\frac{1}{m_N}\right]^{\frac{1}{2}}\frac{760}{P}\frac{T}{273.2}\frac{1}{N}\frac{t_D E}{L}$$

where Ω is the CCS value. This value is then made mass and charge independent (Ω'), which results in a modified Mason-Schamp equation:

$$\Omega' = \frac{18\pi^{1/2}}{16}\frac{1}{k_B T^{1/2}}\frac{760}{P}\frac{T}{273.2}\frac{1}{N}A(t_D)^B$$

where A and B are experimentally determined using an external calibrant.

In all CCS calculations a solution of polyalanine was used as the CCS calibrant using values from Dr. Clemmer's database at Indiana University.[16] It is recognized that using polyalanine as a calibrant for cyclodextrin is not ideal due to the molecules' different structural attributes.[14b] However given Dr. Clemmer's extensive database regarding polyalanine and a lack of molecules similar to cyclodextrin's structure and size in the literature, polyalanine is the best choice as a calibrant for the experiment described.

CHAPTER 4

RESULTS

Positive mode investigation of cyclodextrins

Alpha-, beta-, and gamma-cyclodextrins expectedly had similar spectra, as the only difference between the three compounds is the number of glucose monomers within the oligosaccharide (six, seven, and eight monomers respectively). For all three compounds, the most intense signal was the $[M+K+H]^{2+}$ adduct. Likewise, in the 1+ charge state trend line the most intense peak comes from the $[M+Na]^{+}$ adduct, the 2+ charge state's most intense peak was the $[M+K+H]^{2+}$, and the triply charged charge states most intense peak was a result of the $[4M+2K+H]^{3+}$ adduct.

Amino-beta-cyclodextrin had slightly different spectra than the unfunctionalized cyclodextrins. The most intense peak in the IM-MS spectrum is from the 1+ in opposition to the unfunctionalized spectra; the peak is the $[M+H]^{+}$. Clearly this change is due to the basic nature of the amino moiety added to the cyclodextrin. The most intense peak in the 2+ charge state follows true to it's unfunctionalized counterparts as $[M+K+H]^{2+}$, however the 3+ charge state deviates from the trend set with alpha-, beta-, and gamma-cyclodextrin again. The most intense peak in this spectrum was the $[6M+3H]^{3+}$. Again, the amino moiety is showing a preference for protonation over adduction with alkali ions.

Hydroxypropyl-beta-cyclodextrin showed almost exclusively the 2+ charge state. The 1+ and 3+ charge states were too weak to be able to definitely assign the peaks. The 2+ charge state however clearly showed both the $[M+K+H]^{2+}$ and $[2M+K+H]^{2+}$ ions in the spectrum.

Negative Mode investigation of Cyclodextrins

Both alpha and beta cyclodextrin had their most abundant species as $[M-H]^{1-}$, however gamma's most intense peak was the doubly charged dimer, $[2M-2H]^{2-}$. For the doubly charged anionic state, beta and gamma cyclodextrin shared the same $[2M-2H]^{2-}$ base peak, while alpha-cyclodextrin's base peak was $[3M-2H]^{2-}$. The triply charged state however, was different for each cyclodextrin, as indicated in Figures 6-8.

Amino-beta-cyclodextrin was more similar to the unfunctionalized cyclodextrins in negative mode than positive mode. As indicated by Figure 9 the base peak for the spectrum was $[M-H]^{1-}$. For the 2- charge state the base peak was $[2M-2H]^{2-}$, and for the triply charged 3- state the base peak was $[5M-3H]^{3-}$.

Hydroxypropyl-beta-cyclodextrin showed a very different range of charge states than those observed in positive mode. Both the 1-, and the 2- had identifiable peaks, although the triply charged state, again, did not have identifiable peaks. The base peak of the spectrum was $[M-H]^{1-}$ and the base peak of the 2- charge state was $[2M+K+Na-4H]^{2-}$.

Lipid/alpha-cyclodextrin non-covalent inclusion complexes

In these experiments three lipid/alpha-cyclodextrin non-covalent inclusion complexes were investigated. The lipids tested were sphinganine, sphingosine, and four phosphatidylcholines, of which only one complex with alpha-cyclodextrin was successfully detected.

Sphinganine was detected as $[M+H]^+$ with a drift time of 3.80ms through the T-Wave cell. The sphinganine complex was detected as $[M+\alpha CD+H]^+$ with a drift time of 7.95ms.

Similarly, sphingosine was detected as its $[M+H]^+$ ion with a drift time of 3.88ms. The sphingosine complex with alpha-cyclodextrin was detected at 8.09ms, and thus a shift in drift time of 4.21ms as the monomeric $[M+\alpha CD+H]^+$.

The final complex investigated was with 1-Palmitoyl-2-Myristoyl-*sn*-Gylcero-3-phosphocholine (PMG). The phosphocholine was detect at 7.95ms as the $[M+H]^+$ ion. The complex with alpha-cyclodextrin was detected as a doubly charged species, and thus as a substantially short drift time than the lipid alone, as opposed to the other lipids whose complex drifted slower through the T-wave cell than the uncomplexed lipid; the complex was detected at 2.37ms, as the $[M+\alpha CD+H+K]^{2+}$ adduct.

Cholesterol/hydroxypropyl-beta-cyclodextrin inclusion complex

HP-βCD and cholesterol were added to a solution of 2:1 methanol/chloroform. Detection of a complex between the two was unsuccessful, despite its prescience in prior literature.[17] Still, dehydrated cholesterol was detected at m/z 369.3621. At a wave height of 30V, dehydrated cholesterol's drift time was 1.75ms; this corresponds to a CCS of 134$Å^2$.

Effect of wave height on CCS Values

In addition to the experiments involving cyclodextrins as shift reagents, wave heights of the travelling wave applied to the drift cell were varied to determine the effect

on CCS values. As shown in Table 11 the height of the electric field wave can dramatically affect the calculated CCS value of not only lipids, but complexes as well. This is demonstrated by the ratio of 40V CCS over 25V CCS the lipids and complexes underwent as the wave height was increased. The PMG ion changed the least by increasing by a ratio of 1.06, whereas the PMG complex changed the most by decreasing by a ratio of 0.44. Additionally, a wave height of 25 V, a CCS of 134 $Å^2$ for sphingosine, 223 $Å^2$ for the complex with alpha-cyclodextrin were obtained, while at 40 V sphingosine showed a CCS value of 143 $Å^2$, and its complex 187$Å^2$. These changes in CCS with wave height variations may be from the ion's dipole aligning with the electric field in the T-wave.[18]

CHAPTER 5

DISCUSSION

Positive mode investigation of cyclodextrins

Five cyclodextrin molecules were investigated by ESI as their different charge states, and adducts were separated by T-Wave IMS and detected by MS. All of the spectra were very complex due to various alkali adducts at each charge state, but the IM stage aided in spectral investigation. Identified species are shown in Tables 1-10. Each line going from the origin in the bottom right and leading to and to the right indicates a different charge state family, unfolding to a spectrum that coincidently resembles a "fan" surrounding the $[3nM+nAlkali]^{n+}$ vertical line (approximately at 3000m/z for the alpha-cyclodextrin spectrum), where n is a whole number. As seen from this trend, lines corresponding up to 8+ charge states seem to have been faintly detected, however the adducts corresponding to these peaks are too weak to be correctly identified in the MS spectrum. Thus, because charge states 4+ and higher are not resolvable, only charge states 1+ though 3+ are discusses herein; in negative mode charge state 4- and higher are not resolvable, thus like positive mode, only charge states 1- through 3- will be discussed.

Of the data obtained, CCS values were not directly correlated to the mass of the adduct. For instance, the $[M+Na]^{+}$ ion was substantially larger than the $[M+K+H]^{2+}$ ion in the unfunctionalized CD's and in Amino-βCD; the singly charged ion is larger by at least 30 $Å^2$ in all cases, and as high as 82 $Å^2$ in the case of αCD. The explanation of this observation depends on where the charges lie in space. If the two charges were close to each other, a strong dipole could align with the electric field causing a smaller CCS with the drift gas.[18] Dipole alignment is a phenomenon where the ion's dipole aligns with the

electric field in the T-Wave cell, if the electric field can do enough work on the ion to overcome the rotational energy of the ion.[18] Depending on the direction of the ion's dipole, the ion may lie either more parallel or perpendicular to the drift region, giving either a smaller or larger CCS value, respectively.[18] However, if the charges were too close to each other, Coulombic repulsion would cause the ion to expand and result in a larger CCS. Thus, the charges must be moderately distant from each other in order to maximize the ions dipole with minimal Coulombic repulsion to have the ion's dipole align with the T-Wave electric field and result in a smaller CCS. Molecular dynamic calculations to determine the placement of charges on the ions have not been performed.

Additionally, the CCS of the $[4M+2K+H]^{3+}$ complexes was only about twice the size of any of the monomer adducts in the α, β , and γCD spectra. These unexpected trends in the CCS of the ions again point to dipole alignment within the T-Wave cell.

HP-βCD had a very different spectrum than the other cyclodextrins, mainly because of when βCD is functionalized to HP-βCD. The functionalization replaces a hydroxyl group with a 2-hydroxypropyl group; additional functionalization may occur at the hydroxyl on the 2-hydroxypropyl resulting in a polymerization of 2-hydroxypropyl moieties on cyclodextrin.[17] The process is non-regioselective instead of a simple, single substitution, so HP-βCD appears as several polymeric envelopes in its spectra (the base peak in the 2+ spectrum was the result of the addition of seven 2-hydroxypropyl groups).

Aside from this feature, the most peculiar part to the spectrum was the extreme intensity of the doubly charged state compared to the 1+ and 3+ states. The 2+ charge state was about 100 times more intense than that of the 1+ state, and 3+ was so weak that resolution suffered and peaks could not be assigned. As a comparison, in all the other

spectra the 2+ and 1+ states were at least within an order of magnitude to each other, and the 2+ and 3+ were within 2 orders of magnitude to each other. A theoretical explanation for this observation may be attainable through molecular dynamic simulations, however these have not been performed. However, it is clear that this HP-βCD is more stable as a 2+ cation than any of the other CDs investigated here.

Negative Mode investigation of Cyclodextrins

In negative mode, CCS values were not obtained, as the polyalanine T-Wave calibrant did not ionize effectively using negative mode ESI. Additionally, the spectra in negative mode were generally less intense than their positive mode analogues.

For the unfunctionalized CD's and Amino-βCD the negative mode spectra were relatively predictable, and thus they will not be discussed in depth. It was interesting that alkali cation contaminates complicated the negative mode spectra as well. The only anion that adducted with the CDs was chloride, and all other negative charges accumulated were from the loss of a hydroxyl proton. Additionally, no adduct was identified with both halogen anions, and alkali metal cations; all were either halide adducts, or alkali adducts with the loss of one to several protons.

HP-βCD again had a complex spectrum compared to the other CD's due to its functionalization process. In negative mode the 1- charge state was about an order of magnitude more intense than the 2- state; again the 3- was too weak to be detected.

Lipid/alpha-cyclodextrin non-covalent inclusion complexes

In addition to spectra of various cyclodextrins, several lipids were successfully complexed and ionized. Sphinganine and sphingosine are sphingolipids typically found in brain tissue, and their glycosylated counterparts are of specific interest in NPC.[1b] As shown in Figures 11-12, the addition of cyclodextrin greatly changes the spectrum. The complexes have very different drift times as compared to the naked lipids, and both were detected as a singly charged ion. Because of the complex formation, the two lipids had similar cross sections (223 and 225 $Å^2$ respectively), and thus like their naked ions, the complexes would be very difficult to resolve in the IMS spectrum alone.

The other lipid successfully detected as a CD non-covalent complex, PMG, is a phosphatidylcholine. This was detected as a doubly charged ion, and because of this the complexes drift time was shorter than the naked ion, unlike the sphingolipids. The additional charge on the phosphatidylcholine complex is likely on the lipid itself. The lipid is zwitterionic, with a cationic quaternary amine and an anionic phosphate moiety. The additional charge is likely on the phosphate group, neutralizing the moiety and making the net charge of the ion 1+. Because the two classes of lipids were shifted in opposite directions in the IM spectrum, this may mean that different class of lipids may be able to be separated using a single cyclodextrin. In order for this to be the case, all lipids of the same class would have to ionize to the same charge state. However, more lipid complexes would need to be detected to draw a definitive conclusion.

Cholesterol/hydroxypropyl-beta-cyclodextrin inclusion complex

As noted before, a complex between cholesterol and HP-βCD was not detected. This is most likely due to the complex dissociating during the ESI process, as the complex has been detected using a multimode electrospray ionization/ atmospheric pressure photoionization (ESPI) source.[17] Experiments in an effort to detect the complex used a capillary voltage as low as 2kV in order to avoid dissociation were also unsuccessful. Therefore, the van der Waal forces holding the cholesterol within the cyclodextrin must be significantly weaker than the forces holding the other complexes reported here together, as those complexes were detected using a capillary voltage of 4kV. Additionally, the previously reported detection of the complex used very high concentrations (1mM), whereas in the experiments preformed here were using concentrations of 60μM cholesterol and 250μM HP- βCD.

Still, cholesterol was successfully ionized by ESI with minimal fragmentation. Cholesterol was observed as $[M\text{-}H_2O+H]^+$, and had a CCS of 134 at 30V wave height.

Effect of wave height on CCS Calculations

In addition to the previous survey experiments, the effect of the height of the travelling wave on the conformation of several ions and complexes was studied in order to examine changes in the corresponding CCS values. In addition to the lipids and complexes tested, leucine-enkephalin (Leu-Enk) was tested as well. This was done as a way to ensure our calibration produced CCS values that matched literature results. The data obtained from these experiments show Leu-enk had a CCS of 126Å^2 at 25 V wave height, with previous reports indicating anywhere from 150Å^2 to 400Å^2 through

computational models, although a value of 162Å^2 was reported via IMS.[19] The ESI needle was held at 4krV, and thus the protein could have unfolded during ionization leading to a smaller CCS. Additionally, the computational methods employed to calculate the CCS may have been performed assuming a different drift gas, or in some cases, were extrapolated from data of other proteins like bradykinin.[19c, 19e]

The trend throughout the data is that naked lipids increase in CCS as wave height increases, however than their complexed analogues decrease in CCS as wave height is increase. This is likely due to the rigidity associated with the complexation. Because the hydrocarbon chain on the lipids is inserted in the cyclodextrin ring, the chains have fewer conformations available to them, and are therefore more rigid than their naked counterparts. This gives the ion a more definite shape, and ultimately this manifests itself into an observable dipole alignment, as shown by the various CCS values in Table 11.

The naked ions, without the added rigidity of the cyclodextrin host, have many more conformations available to them. Therefore, the hydrocarbon chain is allowed to rotate, and rapidly change conformation; furthermore, the internal energy of the ion would increase within a higher electric field allowing higher energy rotational state to be reached. These changes would be centered on the charged head group, and therefore the ion would not have a definite dipole, unlike the complexes. Thus dipole alignment is not observed. Instead, there is much less variation in CCS values, shown by the smaller deviations of the naked ions compared to the complexes.

Like the cyclodextrin complexes, dipole alignment was also observable with cholesterol at high wave heights. Cholesterol was the only naked ion observed to decrease in CCS as wave height was increased. Unlike other naked ions, cholesterol has

a rigid polycyclic hydrocarbon structure. This rigidity leads to a fixed dipole on the ion, which then could align with the electric field in the T-Wave cell. As wave height was varied from 25V to 35V the CCS only changed by 2Å^2 (from 136Å^2 to 134Å^2 respectively). However at 40V a significant change in CCS was observed. The CCS decreased to 104Å^2 at 40V, which again is likely due to dipole alignment within the T-Wave cell.

CHAPTER 6

CONCLUSION

Non-covalent inclusion complexes are growing in importance in the pharmaceutical industry as drug delivery agents. In particular, hydroxypropyl-β-cyclodextrin is new approval as a treatment for Niemann-Pick type C has made the detection of lipids and lipid/cyclodextrin complexes nontrivial. In the data presented, detection of these complexes was accomplished via T-Wave-MS; in addition to this CCS values were obtained by the ions corresponding drift time through the T-Wave cell. As shown in Figures 11-13, complexation of the lipids with cyclodextrin shifts their point in the m/z vs. CCS space, which can aid in their detection and spectral interpretation.

In addition, to these findings, evidence of dipole alignment within the T-Wave cell was found. As shown in Table 11, more rigid ions, which would have a fixed dipole, decrease in CCS as wave height is increased; the ratio of CCS at 40V to 25V for these ions was between 0.44 to 0.84. In contrast to this, ions with freer rotations had larger CCS values at increased wave heights, although this increase was less pronounced than the decrease seen in rigid ions. This is likely due to increased internal energy of the ions at higher wave heights, leading to more energetic rotations of the hydrocarbon chain and ultimately a larger CCS.

A complex between cholesterol and HP-βCD was not detected, although dehydrated cholesterol ions were. Therefore, CCS for dehydrated cholesterol were obtained, and subjected to various wave heights within the T-Wave. Again, like the rigid

lipid/cyclodextrin complexes, smaller CCS values were obtained for cholesterol at higher wave heights.

Ion mobility spectrometry is a rapid separations technique increasing in popularity within the MS community. The experiments presented here demonstrate both fundamental aspects of traveling-wave ion mobility mass spectrometry, as well as its applications to biomolecules. As shown, the introduction of shift reagents can aid in spectral interpretations of the complex two-dimensional data. In addition to this, parameters within the T-Wave can greatly affect the CCSs obtained, and should be set carefully to not skew results.

FIGURES

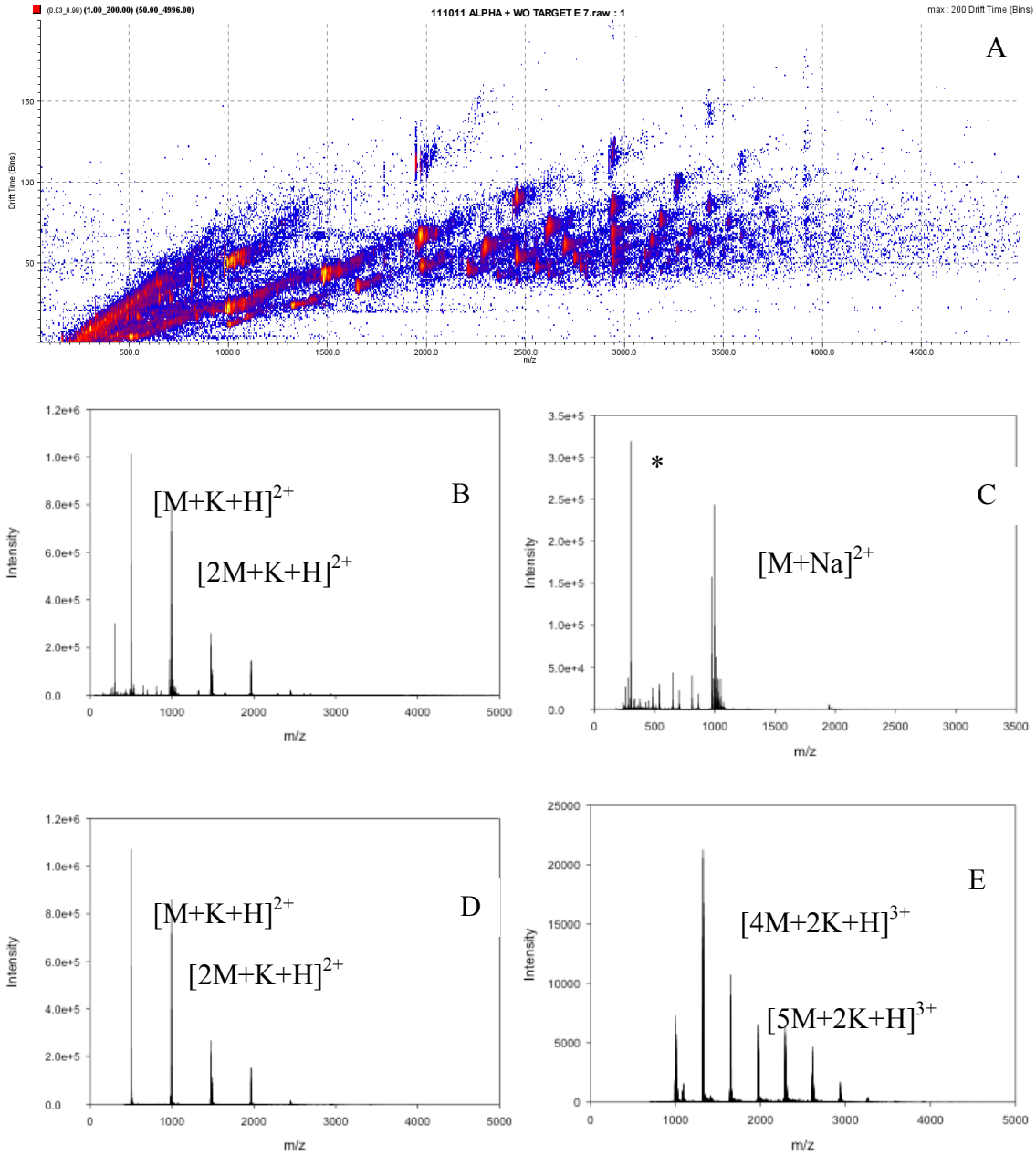

Figure 1: A) IM-MS Spectrum of α-Cyclodextrin. B) MS Spectrum of α-Cyclodextrin; Base Peak $[M+K+H]^{2+}$ CCS: 145 $Å^2$. C) Charge State 1+ from IM-MS Spectrum of α-Cyclodextrin; Base Peak $[M+Na]^{+}$ CCS: 227 $Å^2$ (* m/z=301=[Dibutylphthalate +$Na]^{+}$). D) Charge State 2+ from IM-MS Spectrum of α-Cyclodextrin; Base Peak $[M+K+H]^{2+}$ CCS: 145 $Å^2$. E) Charge State 3+ from IM-MS Spectrum of α-Cyclodextrin; Base Peak $[4M+2K+H]^{3+}$ CCS: 503 $Å^2$.

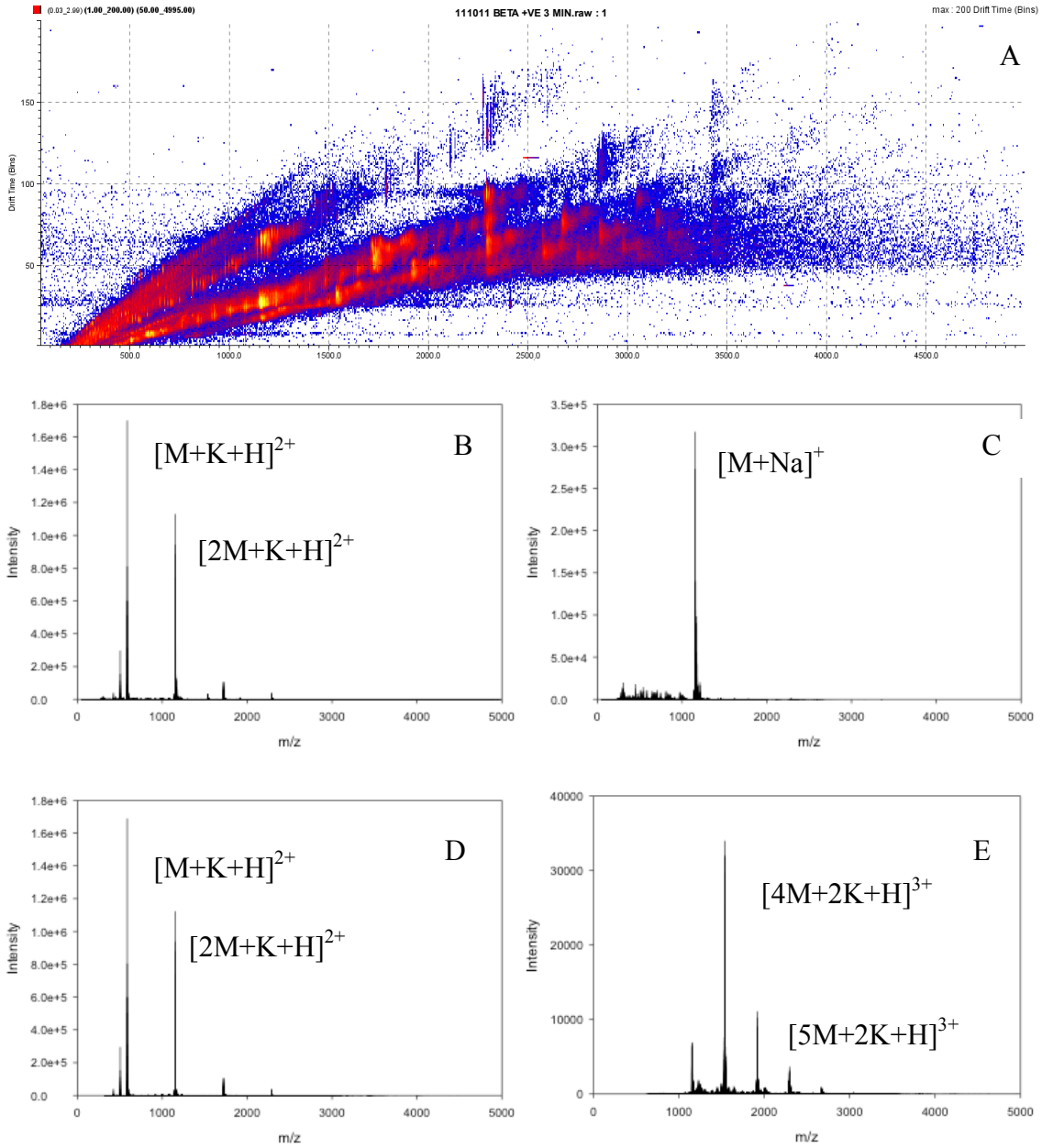

Figure 2: A) IM-MS Spectrum of β-Cyclodextrin. B) MS Spectrum of β-Cyclodextrin; Base Peak $[M+K+H]^{2+}$ CCS: 202 $Å^2$. C) Charge State 1+ from IM-MS Spectrum of β-Cyclodextrin; Base Peak $[M+Na]^{+}$ CCS: 255 $Å^2$. D) Charge State 2+ from IM-MS Spectrum of β-Cyclodextrin; Base Peak $[M+K+H]^{2+}$ CCS: 202 $Å^2$. E) Charge State 3+ from IM-MS Spectrum of β-Cyclodextrin; Base Peak $[4M+2K+H]^{3+}$ CCS: 575 $Å^2$.

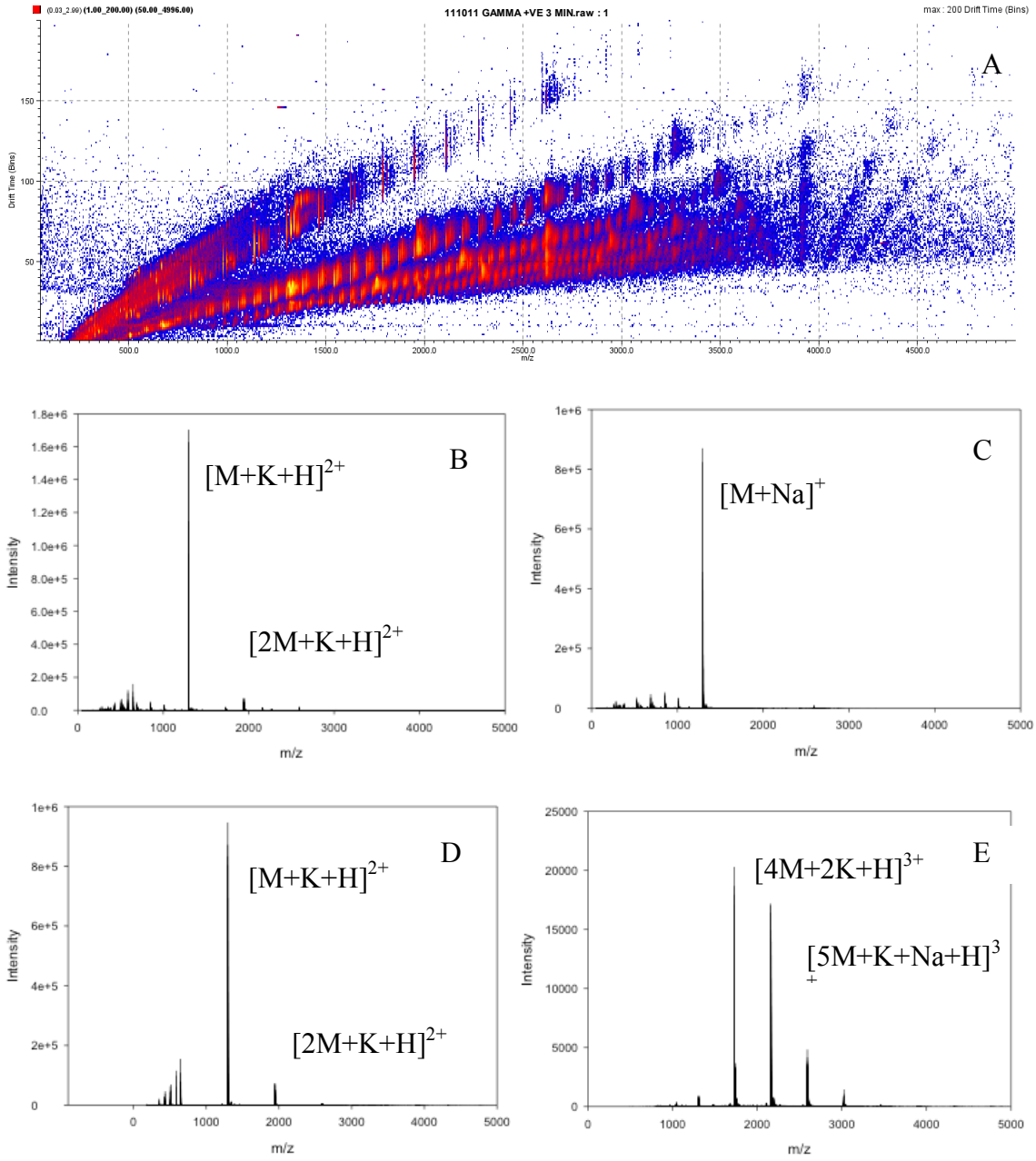

Figure 3: A) IM-MS Spectrum of ɣ-Cyclodextrin. B) MS Spectrum of ɣ-Cyclodextrin; Base Peak $[M+K+H]^{2+}$ CCS: 230 Å^2. C) Charge State 1+ from IM-MS Spectrum of ɣ-Cyclodextrin; Base Peak $[M+Na]^{+}$ CCS: 260 Å^2. D) Charge State 2+ from IM-MS Spectrum of ɣ-Cyclodextrin; Base Peak $[M+K+H]^{2+}$ CCS: 230 Å^2. E) Charge State 3+ from IM-MS Spectrum of ɣ-Cyclodextrin; Base Peak $[4M+2K+H]^{3+}$ CCS: 607 Å^2.

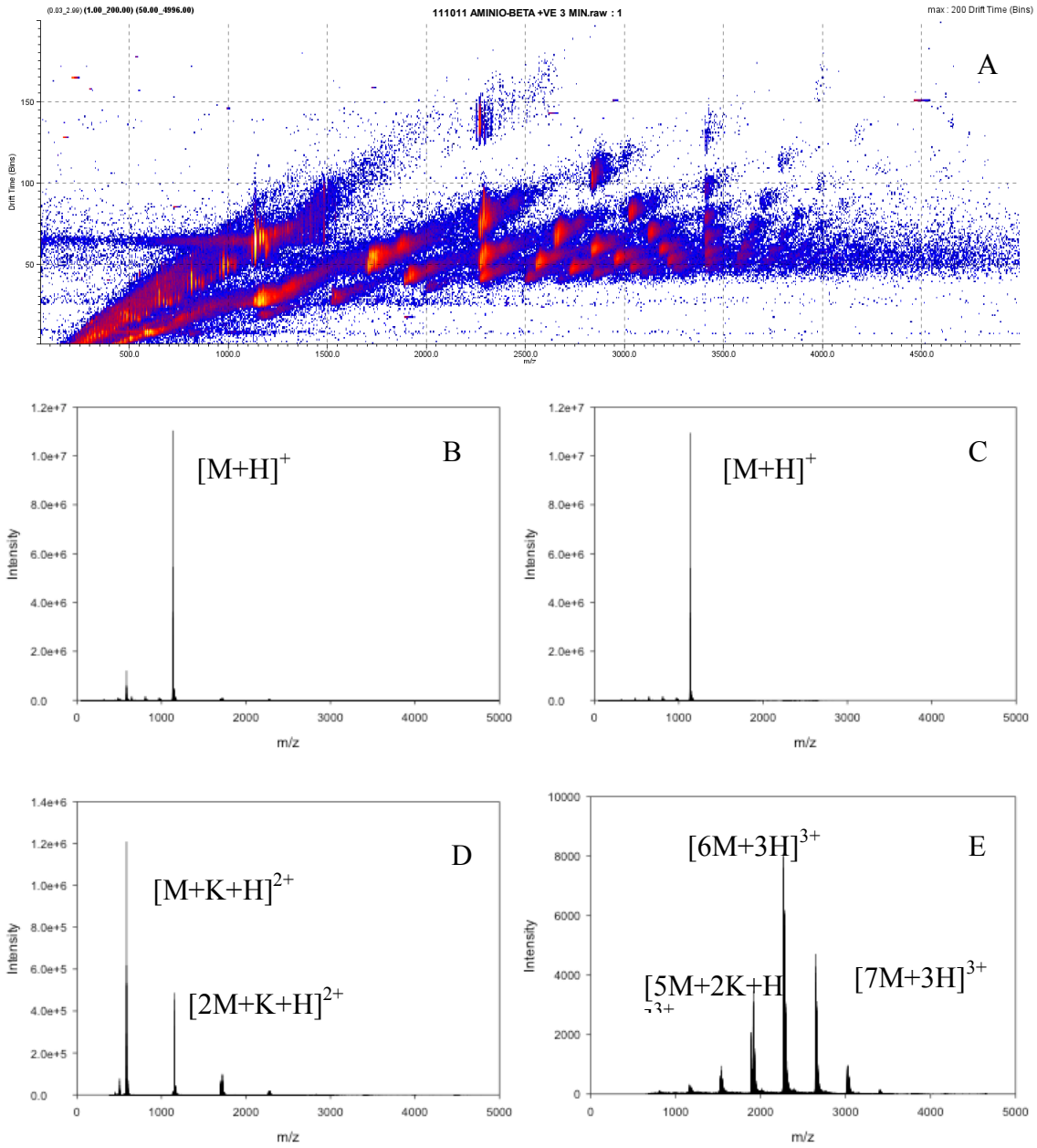

Figure 4: A) IM-MS Spectrum of Amino-β -Cyclodextrin. B) MS Spectrum of Amino-β -Cyclodextrin; Base Peak $[M+H]^+$ CCS: 252 Å^2. C) Charge State 1+ from IM-MS Spectrum of Amino-β -Cyclodextrin; Base Peak $[M+H]^+$ CCS: 252 Å^2. D) Charge State 2+ from IM-MS Spectrum of Amino-β -Cyclodextrin; Base Peak $[M+K+H]^{2+}$ CCS: 211 Å^2. E) Charge State 3+ from IM-MS Spectrum of Amino-β -Cyclodextrin; Base Peak $[4M+3H]^{3+}$ CCS: 689 Å^2.

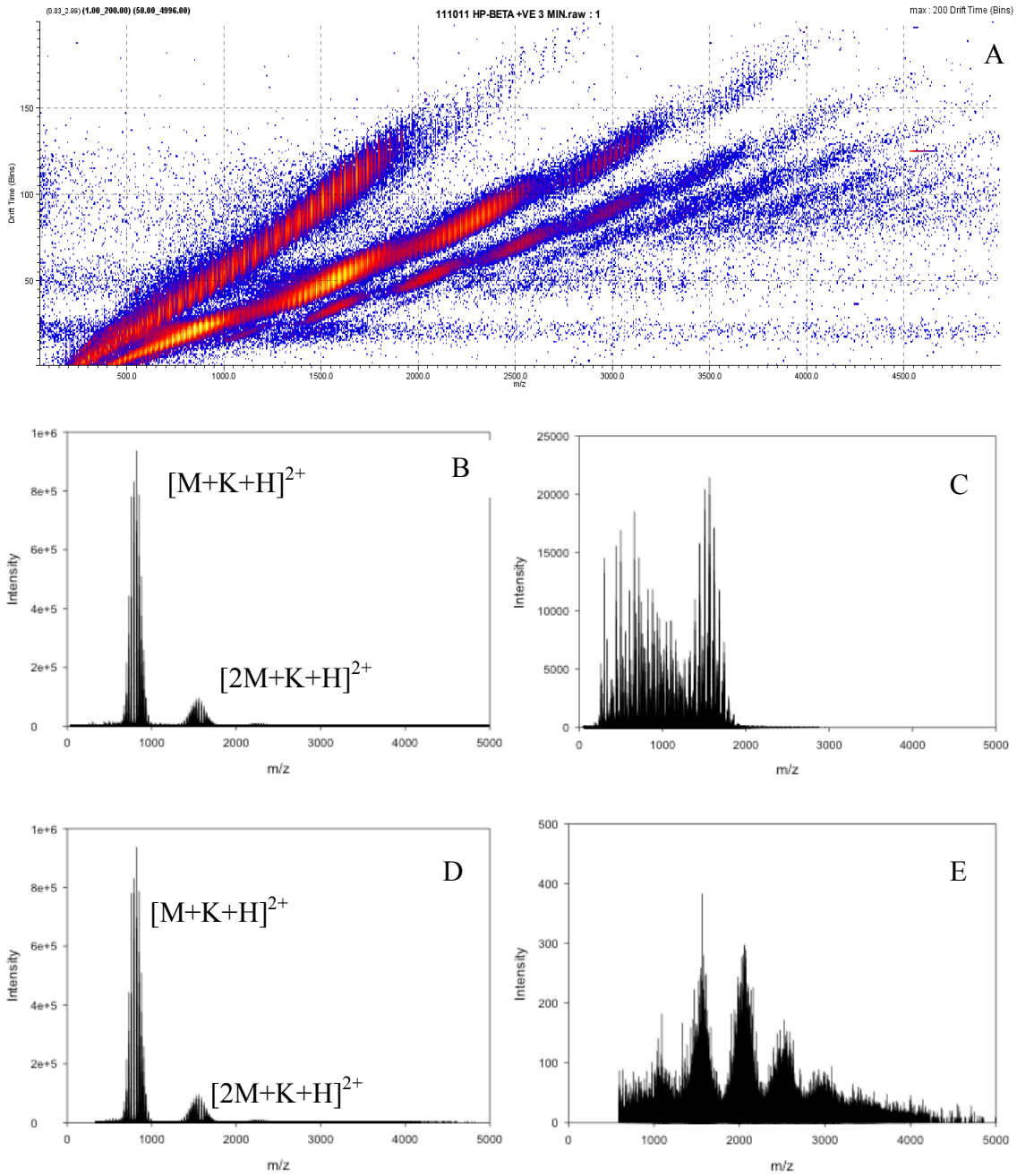

Figure 5: A) IM-MS Spectrum of Hydroxypropyl-β -Cyclodextrin. B) MS Spectrum of Hydroxypropyl-β -Cyclodextrin; Base Peak $[M+H]^+$ CCS: 298 $Å^2$. C) Charge State 1+ from IM-MS Spectrum of Hydroxypropyl-β -Cyclodextrin; Base Peak $[M+H]^+$ CCS: 298 $Å^2$. D) Charge State 2+ from IM-MS Spectrum of Hydroxypropyl-β -Cyclodextrin; Base Peak $[M+K+H]^{2+}$ CCS: 460 $Å^2$. E) Charge State 3+ from IM-MS Spectrum of Hydroxypropyl-β -Cyclodextrin; identifiable species unresolved.

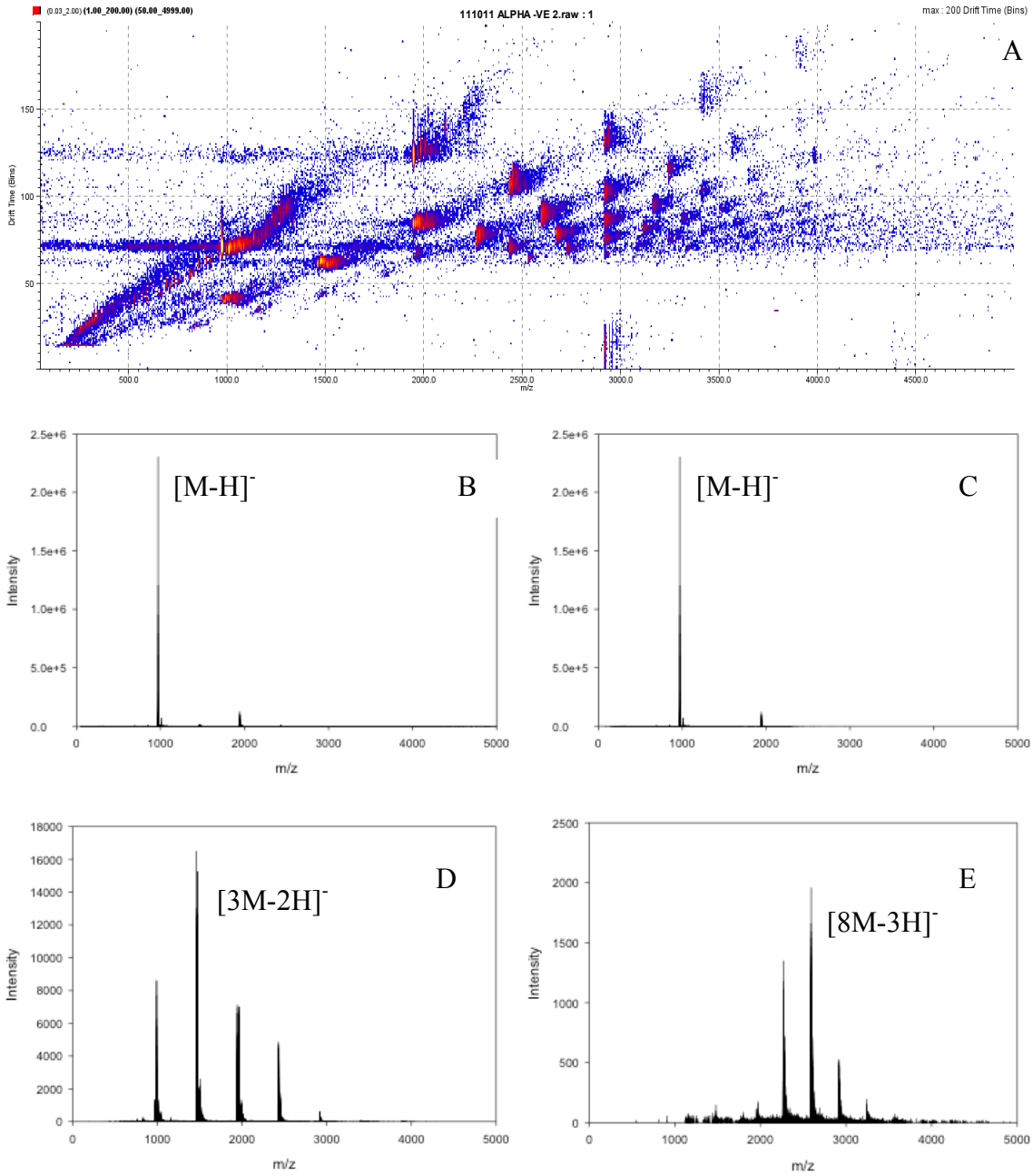

Figure 6: A) IM-MS Spectrum of α-Cyclodextrin in negative mode. B) MS Spectrum of α-Cyclodextrin; Base Peak $[M-H]^-$. C) Charge State 1- from IM-MS Spectrum of α-Cyclodextrin; Base Peak $[M-H]^-$. D) Charge State 2- from IM-MS Spectrum of α-Cyclodextrin; Base Peak $[3M-2H]^{2-}$. E) Charge State 3- from IM-MS Spectrum of α-Cyclodextrin; Base Peak $[8M-3H]^{3-}$.

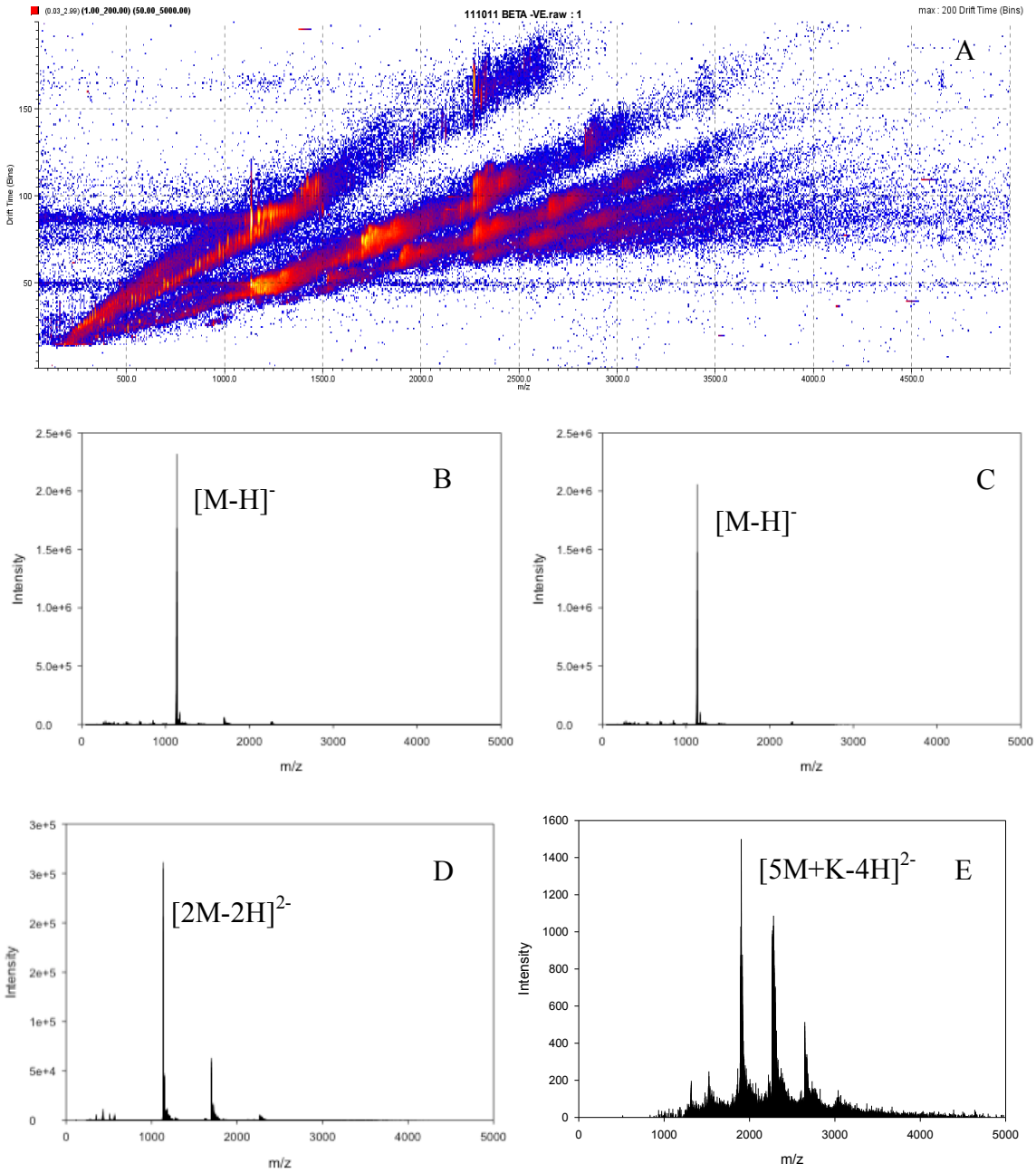

Figure 7: A) IM-MS Spectrum of β -Cyclodextrin in negative mode. B) MS Spectrum of α-Cyclodextrin; Base Peak $[M-H]^-$. C) Charge State 1- from IM-MS Spectrum of β -Cyclodextrin; Base Peak $[M-H]^-$. D) Charge State 2- from IM-MS Spectrum of β -Cyclodextrin; Base Peak $[2M-2H]^{2-}$. E) Charge State 3- from IM-MS Spectrum of β -Cyclodextrin; Base Peak $[5M+K-4H]^{3-}$.

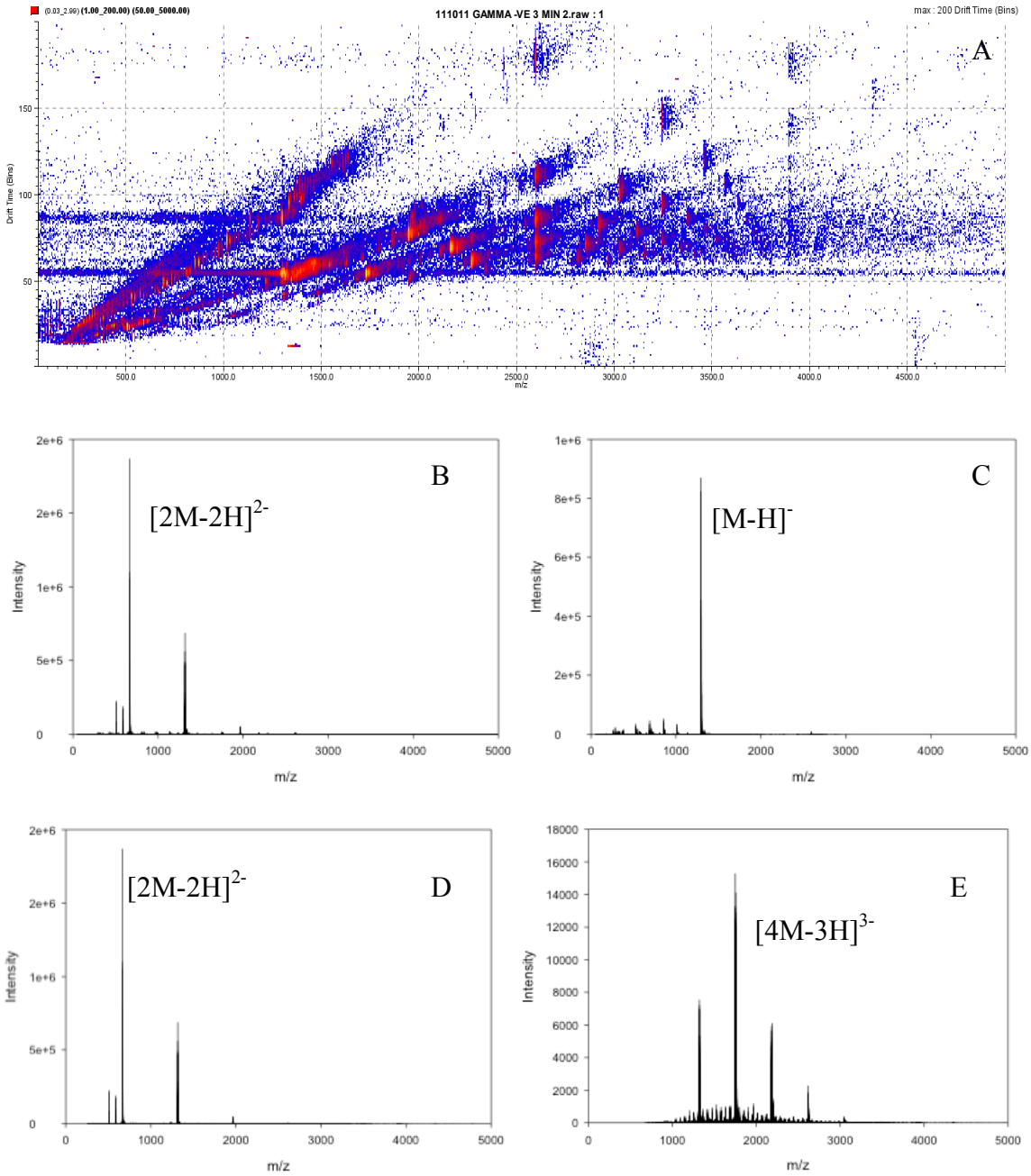

Figure 8: A) IM-MS Spectrum of ɣ -Cyclodextrin in negative mode. B) MS Spectrum of α-Cyclodextrin; Base Peak $[M-H]^-$. C) Charge State 1- from IM-MS Spectrum of ɣ -Cyclodextrin; Base Peak $[M-H]^-$. D) Charge State 2- from IM-MS Spectrum of ɣ -Cyclodextrin; Base Peak $[2M-2H]^{2-}$. E) Charge State 3- from IM-MS Spectrum of ɣ -Cyclodextrin; Base Peak $[4M-3H]^{3-}$.

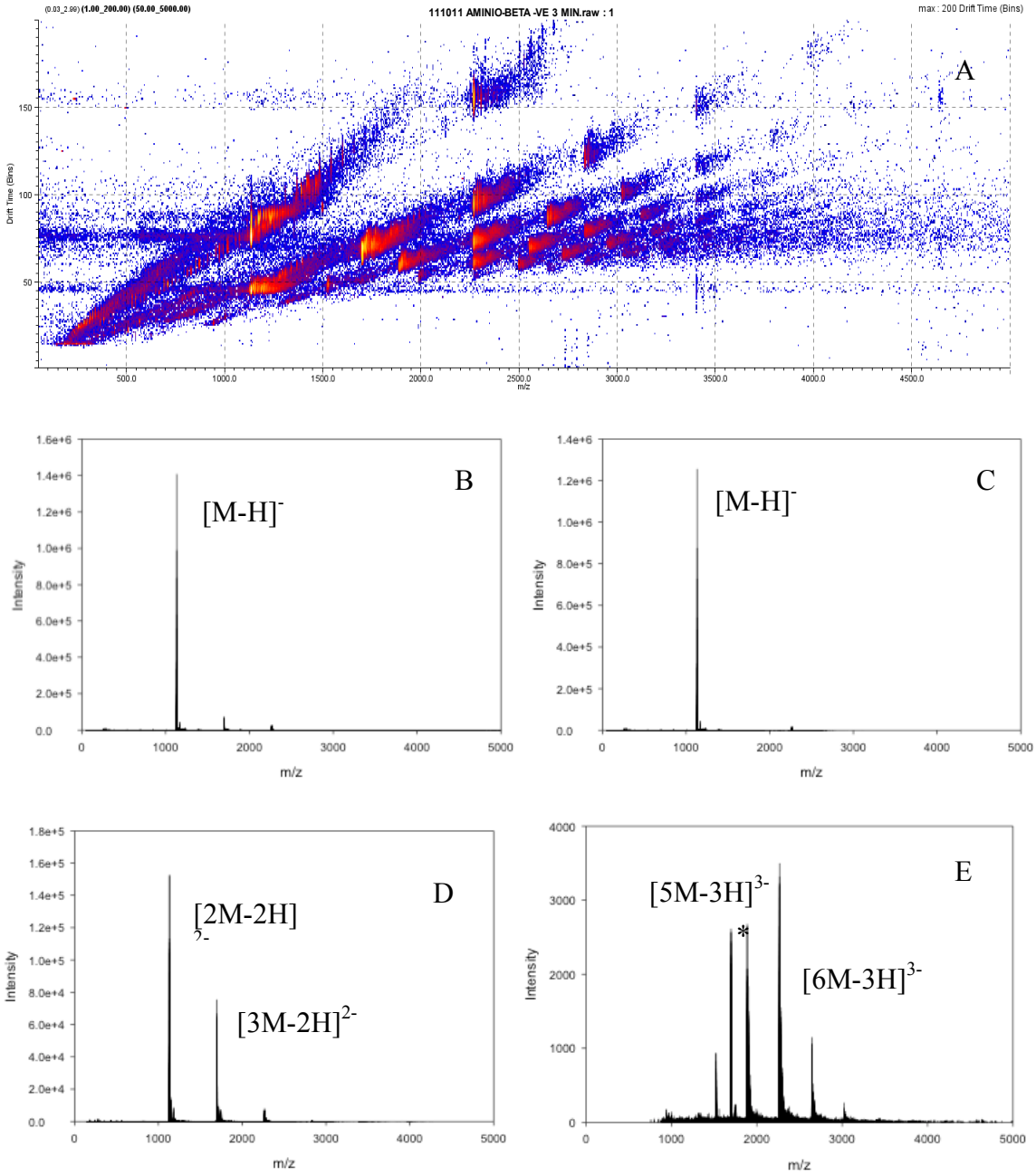

Figure 9: A) IM-MS Spectrum of Amino-β-Cyclodextrin in negative mode. B) MS Spectrum of α-Cyclodextrin; Base Peak $[M-H]^-$. C) Charge State 1- from IM-MS Spectrum of Amino-β-Cyclodextrin; Base Peak $[M-H]^-$. D) Charge State 2- from IM-MS Spectrum of Amino-β-Cyclodextrin; Base Peak $[2M-2H]^{2-}$. E) Charge State 3- from IM-MS Spectrum of Amino-β-Cyclodextrin; Base Peak $[5M+K-4H]^{3-}$ (*$[3M-2H]^{2-}$).

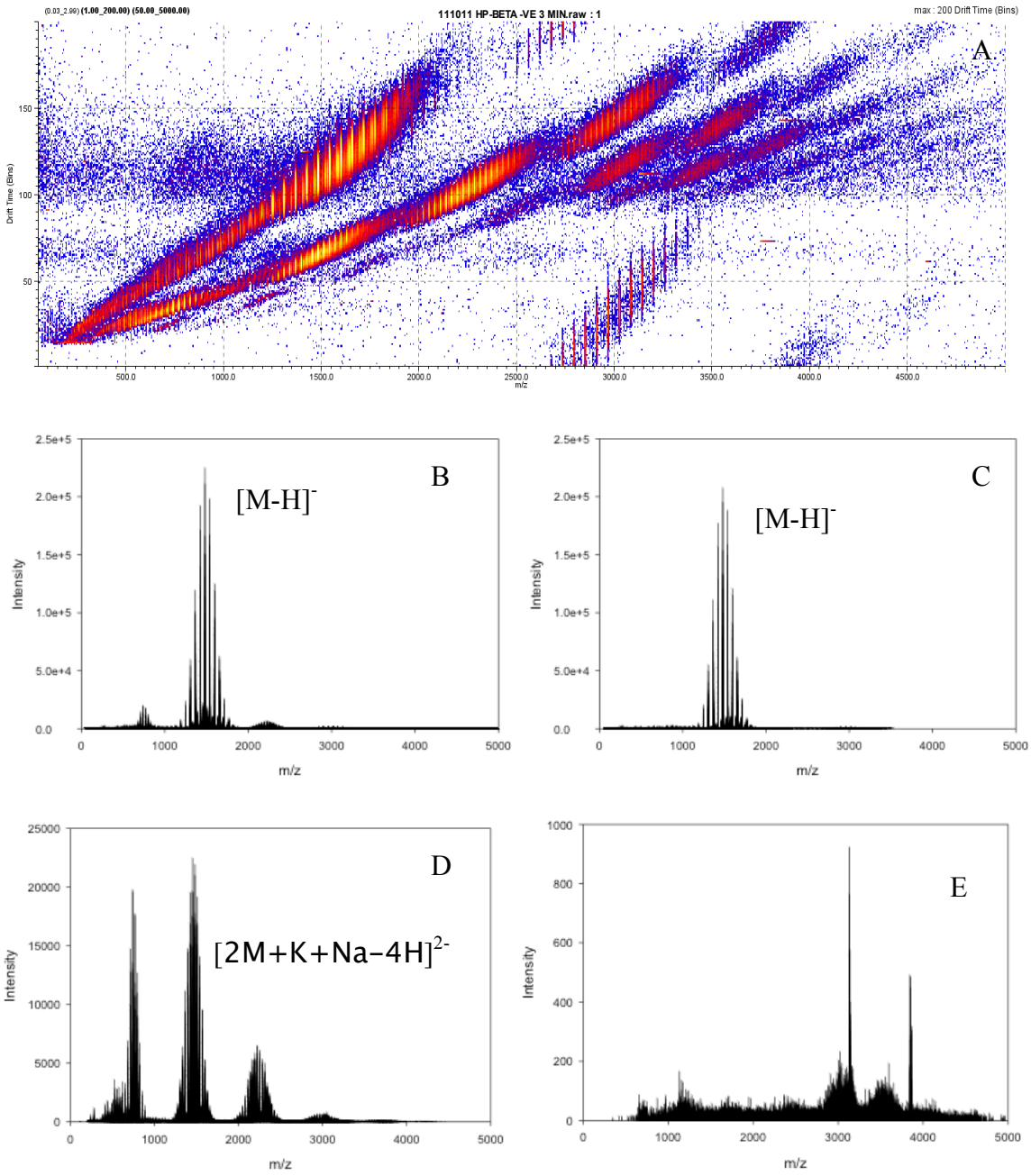

Figure 10: A) IM-MS Spectrum of Hydroxypropyl-β-Cyclodextrin in negative mode. B) MS Spectrum of Hydroxypropyl -β -Cyclodextrin; Base Peak $[M-H]^-$. C) Charge State 1- from IM-MS Spectrum of Hydroxypropyl -β-Cyclodextrin; Base Peak $[M-H]^-$. D) Charge State 2- from IM-MS Spectrum of Hydroxypropyl -β-Cyclodextrin; Base Peak $[2M+K+Na-4H]^{2-}$. E) Charge State 3- from IM-MS Spectrum of Hydroxypropyl -β-Cyclodextrin; Base Peak $[5M+K-4H]^{3-}$.

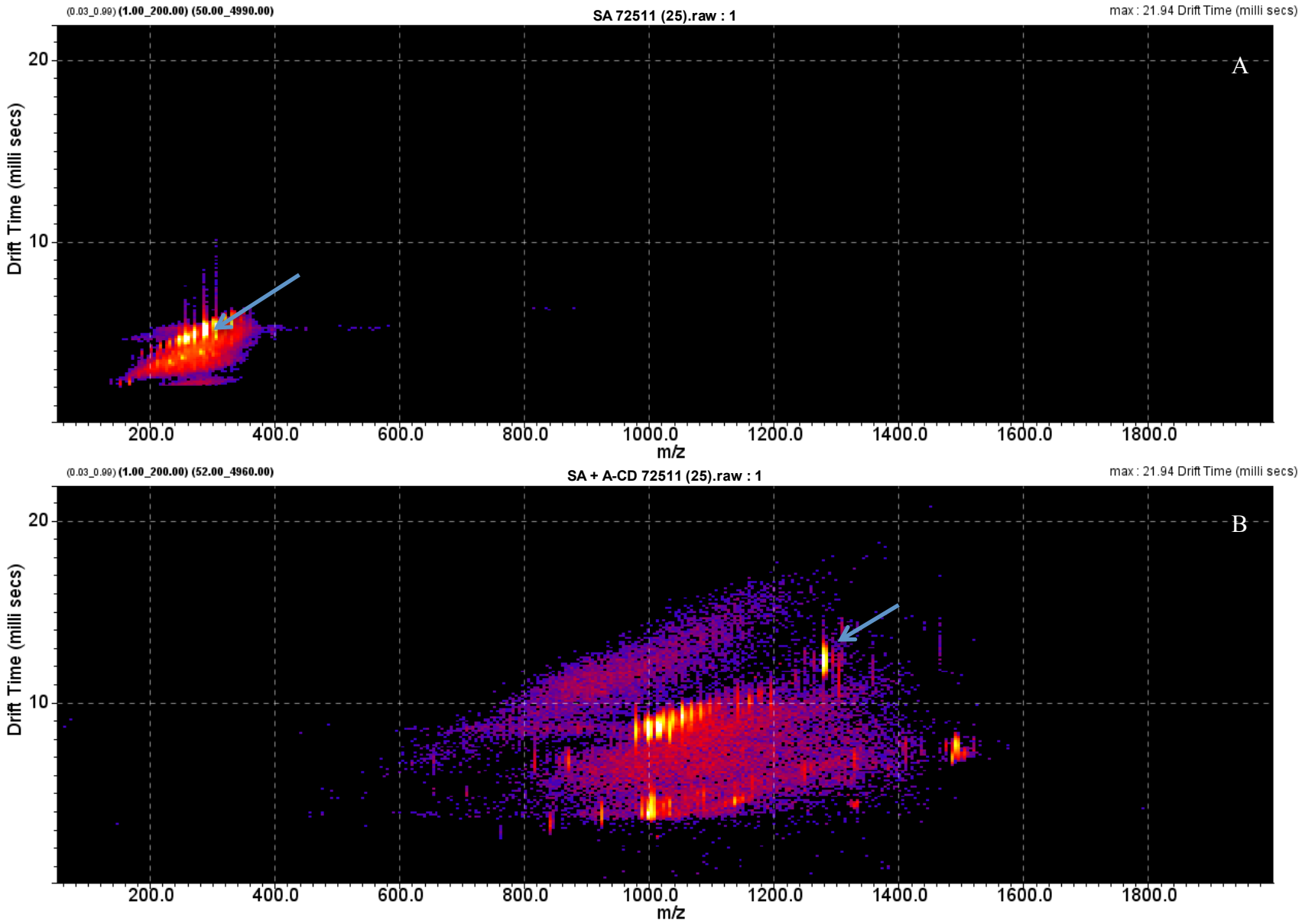

Figure 11) IM-MS Spectrum of Sphinganine without (A) and with (B) α-Cyclodextrin. A) Arrow pointing out Sphinganine alone. B) Arrow pointing out Sphinganine/ α -Cyclodextrin complex

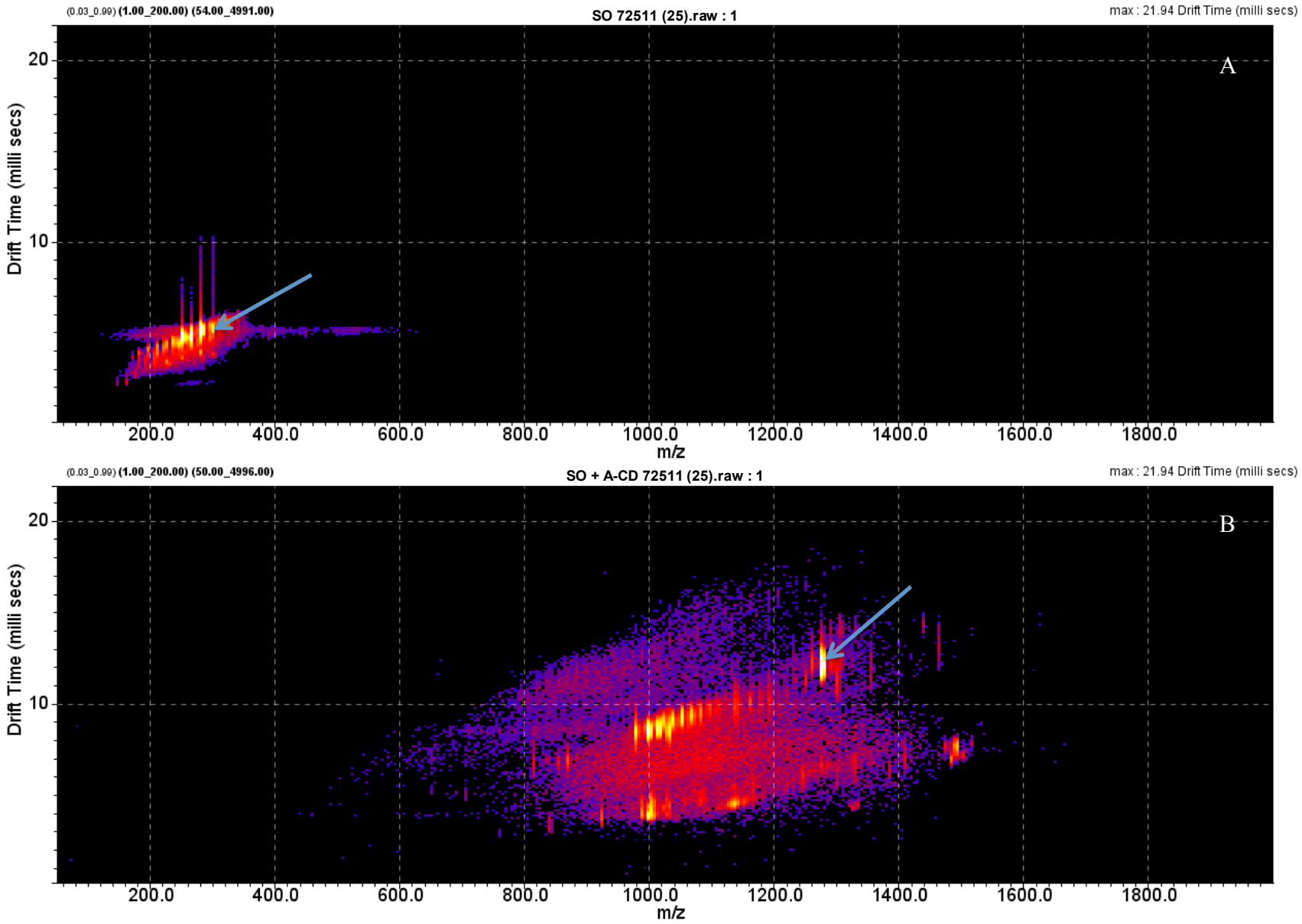

Figure 12) IM-MS Spectrum of Sphingosine without (A) and with (B) α -Cyclodextrin. A) Arrow pointing out Sphingosine alone. B) Arrow pointing out sphingosine/ α -Cyclodextrin complex

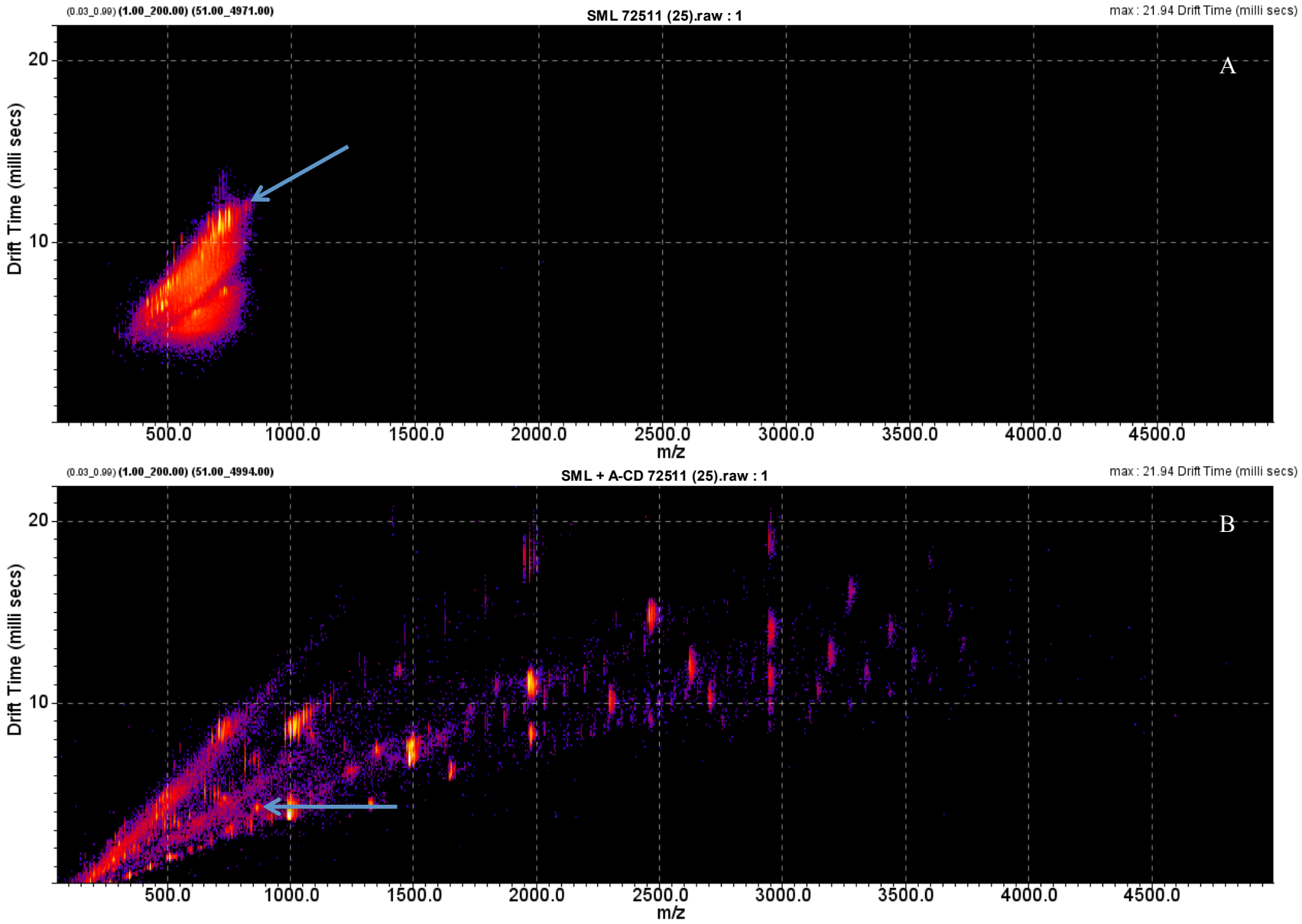

Figure 13) IM-MS Spectrum of PMG without (A) and with (B) Alpha-Cyclodextrin. A) Arrow pointing out PMG alone. B) Arrow pointing out PMG/Alpha-Cyclodextrin complex

TABLES

Table 1: Identified Species in IM-MS Spectrum of Alpha-Cyclodextrin (Positive Mode)

Alpha-Cyclodextrin: Positive Mode								
1+ Charge State			2+ Charge State			3+ Charge State		
Observed m/z	Identity	CCS (Å^2)	Observed m/z	Identity	CCS (Å^2)	Observed m/z	Identity	CCS (Å^2)
973.3710	M+H	226	506.1640	M+K+H	145	993.1070	3M+K+Na+H	368
995.3520	M+Na	227	984.3590	2M+Na+H	317	998.6620	3M+2K+H	372
1011.3320	M+K	229	992.3500	2M+K+H	314	1009.3190	3M+2K+$MeOH_2$	372
1945.7680	2M+H	314	1000.3330	2M+Na+$MeOH_2$	323	1322.7972	4M+2K+H	503
1967.7360	2M+Na	314	1478.5250	3M+K+H	417	1646.9200	5M+2K+H	598
			1470.5410	3M+Na+H	435	1652.2590	5M+K+Na+$MeOH_2$	591
			1486.5300	3M+Na+$MeOH_2$	437	1971.0700	6M+2K+H	679
			1964.7150	4M+K+H	514	1976.3490	6M+K+Na+$MeOH_2$	682
			2450.9300	5M+K+H	583	2290.1820	7M+K+Na+H	740

Table 2: Identified Species in IM-MS Spectrum of Beta-Cyclodextrin (Positive Mode)

Beta-Cyclodextrin: Positive Mode								
1+ Charge State			2+ Charge State			3+ Charge State		
Observed m/z	Identity	CCS (Å^2)	Observed m/z	Identity	CCS (Å^2)	Observed m/z	Identity	CCS (Å^2)
1135.4810	M+H	244	587.2170	M+K+H	202	1155.4530	3M+K+Na+H	504
1157.4580	M+Na	255	1154.4580	2M+K+H	354	1160.7740	3M+2K+H	442
1173.4280	M+K	254	1146.4580	2M+H+Na	358	1538.9380	4M+2K+H	575
			1721.7020	3M+K+H	474	1917.1090	5M+2K+H	690
			2288.9280	4M+K+H	590	2295.2640	6M+2K+H	752

Table 3: Identified Species in IM-MS Spectrum of Gamma-Cyclodextrin (Positive Mode)

Gamma-Cyclodextrin: Positive Mode								
1+ Charge State			2+ Charge State			3+ Charge State		
Observed m/z	Identity	CCS (Å^2)	Observed m/z	Identity	CCS (Å^2)	Observed m/z	Identity	CCS (Å^2)
1319.5580	M+Na	260	668.2560	M+K+H	230	1310.2290	3M+K+2H	487
1297.5640	M+H	260	660.2740	M+Na+H	244	1322.8610	3M+2K+H	493
1335.5370	M+K	267	1316.5460	2M+K+H	381	1749.7450	4M+K+Na+H	597
			1297.5640	2M+2H	376	1742.4260	4M+K+2H	584
			1324.5294	2M+$MeOH_2$+Na	396	1755.0660	4M+2K+H	607
						2181.9220	5M+K+Na+H	689
						2187.2500	5M+2K+H	675

Table 4: Identified Species in IM-MS Spectrum of Amino-β-Cyclodextrin (Positive Mode)

Amino-β-Cyclodextrin: Positive Mode								
1+ Charge State			2+ Charge State			3+ Charge State		
Observed m/z	Identity	CCS (Å^2)	Observed m/z	Identity	CCS (Å^2)	Observed m/z	Identity	CCS (Å^2)
1134.5100	M+H	252	586.7310	M+K+H	211	1889.8580	5M+3H	627
1156.4920	M+Na	255	578.7380	M+Na+H	208	1915.4640	5M+2K+H	642
1172.4560	M+K	256	605.7040	M+2K	213	2268.0380	6M+3H	689
2268.0380	2M+H	340	1134.5100	2M+2H	362	2275.0950	6M+Na+2H	695
			1144.9650	2M+Na+H	354	2280.6820	6M+K+2H	714
			1153.4790	2M+K+H	357	2645.8955	7M+3H	770
			1172.4560	2M+2K	362	2658.5142	7M+K+2H	778
			1701.2650	3M+2H	454			
			1712.2730	3M+Na+H	455			
			1720.2530	3M+K+H	466			
			1739.2360	3M+2K	472			

Table 5: Identified Species in IM-MS Spectrum of 2-Hydroxypropyl-β-Cyclodextrin (Positive Mode)

2-Hydroxypropyl-β-Cyclodextrin: Positive Mode					
1+ Charge State			2+ Charge State		
Observed m/z	Identity	CCS ($Å^2$)	Observed m/z	Identity	CCS ($Å^2$)
1563.7974	M+Na	303	1552.7968	2M+Na+H	459
1579.7809	M+K	302	1560.7935	2M+K+H	460
1541.8177	M+H	298	1568.7759	2M+Na+$MeOH_2$	462
			790.3770	M+K+H	303
			782.3909	M+Na+H	303
			2323.2219	3M+Na+H	577
			2331.2078	3M+K+H	578
			2339.1863	3M+Na+$MeOH_2$	579
			3101.6274	4M+K+H	680

Table 6: Identified Species in IM-MS Spectrum of Alpha-Cyclodextrin (Negative Mode)

Alpha-Cyclodextrin: Negative Mode								
1- Charge State			2- Charge State			3- Charge State		
Identity	Molecular Weight	Observed Monoisotopic Peak	Identity	Molecular Weight	Observed Monoisotopic Peak	Identity	Molecular Weight	Observed Monoisotopic Peak
M-H	971.837	971.3961	2M-2H	1944.682	971.3824	7M-3H	6806.892	2267.9124
M+Cl	1008.298	1007.3691	2M+Na-3H	1965.656	982.3918	7M+Na-4H	6828.874	Not Resolved
2M-H	1944.682	1943.792	2M+K-3H	1981.765	990.3665	7M+K-4H	6844.982	2280.6055
2M+Na-2H	1966.664	1965.7617	2M+K+Na-4H	1030.902	1001.372	8M-3H	7779.737	2592.1352
2M+Cl	1981.143	1979.7767	3M-2H	2916.520	1457.5961	8M+Na-4H	7801.719	Not Resolved
			3M+Na-3H	2961.491	1468.5789	8M+K-4H	7817.828	2604.7456
			3M+K-3H	2954.610	1476.5615	9M-3H	8752.582	Not Resolved
			3M+K+Na-4H	2976.592	1487.5648	9M+Na-4H	8774.564	Not Resolved
			3M+2K+Na-5H	3014.682	1506.5879	9M+K-4H	8790.673	Not Resolved
			4M-2H	3889.365	1943.792			
			4M+Na-3H	3911.347	1954.7904			
			4M+K-3H	3927.455	1962.7595			
			4M+2K+Na-5H	3987.527	1992.788			
			5M-2H	4862.210	2430.0181			
			5M+Na-3H	4884.192	2440.9753			
			5M+K-3H	4900.300	2448.9932			

Table 7: Identified Species in IM-MS Spectrum of Beta-Cyclodextrin (Negative Mode)

Beta-Cyclodextrin: Negative Mode								
1- Charge State			2- Charge State			3- Charge State		
Identity	Molecular Weight	Observed Monoisotopic Peak	Identity	Molecular Weight	Observed Monoisotopic Peak	Identity	Molecular Weight	Observed Monoisotopic Peak
M-H	1133.978	1133.4542	M-2H	1132.970	566.2231	5M+Na-4H	5693.888	1897.0618
M+Cl	1170.438	1169.4298	2M-2H	2267.956	1133.4542	5M+K-4H	5709.996	1902.3954
2M-H	2268.964	2267.9331	2M+Na-3H	1154.952	1144.4421	5M+K+Na-5H	5731.978	Not Resolved
2M+Na-2H	2290.946	2289.9918	2M+K-3H	2306.046	1152.4248	5M+2K-5H	5748.087	1915.0927
2M+Cl	2305.424	2303.9158	3M-2H	3402.942	1700.6729	6M-3H	6806.892	2267.9124
			3M+Na-3H	3424.924	1711.6665	6M+Na-4H	6828.874	Not Resolved
			3M+K-3H	3441.032	1719.6495	6M+K-4H	6844.982	Not Resolved
			4M-2H	4537.928	2267.9331	6M+K+Na-5H	6866.964	Not Resolved
			4M+Na-3H	4559.910	2278.9153	7M-3H	7941.878	Not Resolved
			4M-H+Cl	4574.388	2285.9309			

Table 8: Identified Species in IM-MS Spectrum of Gamma-Cyclodextrin (Negative Mode)

Gamma-Cyclodextrin: Negative Mode								
1- Charge State			2- Charge State			3- Charge State		
Identity	Molecular Weight	Observed Monoisotopic Peak	Identity	Molecular Weight	Observed Monoisotopic Peak	Identity	Molecular Weight	Observed Monoisotopic Peak
M-H	1296.119	1295.5515	M-2H	1295.111	647.2702	4M-3H	5185.484	1727.7138
M+Cl	1332.579	1331.5212	2M-2H	2592.238	1295.5515	4M+Na-4H	5207.465	1735.0522
2M-H	2593.246	2592.1353	2M+Na-3H	2630.328	1306.5228	4M+K-4H	5223.574	1740.3901
			2M+Cl-H	2628.698	1313.5460	5M-3H	6482.610	2159.9382
			3M-2H	3889.365	2592.1353	5M+Na-4H	6504.592	Not Resolved
			3M+Na-3H	3911.347	2603.1172	5M+K-4H	6520.701	2172.2646
			3M+K-3H	3927.455	2610.6155	6M-3H	7779.737	Not Resolved
			4M-2H	5186.491	1943.8306	7M-3H	9076.864	Not Resolved
			4M+Na-3H	5208.473	1954.8097			
			4M+K-3H	5224.582	1961.8109			

Table 9: Identified Species in IM-MS Spectrum of Amino-β-Cyclodextrin (Negative Mode)

Amino-Beta-Cyclodextrin								
1- Charge State			2- Charge State			3- Charge State		
Identity	Molecular Weight	Observed Monoisotopic Peak	Identity	Molecular Weight	Observed Monoisotopic Peak	Identity	Molecular Weight	Observed Monoisotopic Peak
M-H	1132.9933	1132.4833	2M+Na-3H	2287.9685	1143.4813	4M+K-4H	4571.0715	1522.9849
M+Cl	1169.4537	1168.4586	2M+K-3H	2304.0770	1151.4608	5M-3H	5666.9823	1888.1448
2M-H	2266.9945	2265.9771	2M+2K+Na-5H	2364.1493	1181.4766	5M+Na-4H	5688.9642	1895.4631
2M+Na-2H	2289.9843	2287.9790	2M-2H	2265.9866	1132.4833	5M+K-4H	5850.9143	1900.4897
2M+Cl	2303.4549	2301.9863	3M+Na-3H	3421.9697	1710.2203	5M+K+Na-5H	5737.1336	Not Resolved
			3M+2K+Na-5H	3498.1505	1748.2205	5M+2K-5H	5743.1631	Not Resolved
			3M+Cl-H	3436.4482	1717.2218	5M+2K+Na-6H	5765.1450	Not Resolved
			3M-2H	3399.9878	1699.2313	6M-3H	6807.0309	Not Resolved
			4M-2H	4533.9890	2265.998	6M+Na-4H	6822.9654	Not Resolved
			4M+Na-3h	4555.9709	2276.9751	6M+K-4H	6839.0739	Not Resolved
			4M+2K+Na-5H	4632.1517	2314.9004	6M+K+Na-5H	6861.0558	Not Resolved
			4M+Cl-H	4570.4494	2283.967	6M+2K+Na-6H	6899.1462	Not Resolved
			5M-2H	5667.9902	2832.7817	7M-3H	7934.9847	Not Resolved
						7M+Na-4H	7956.9666	Not Resolved
						7M+K-4H	7973.0751	Not Resolved
						7M+2K+Na-6H	8033.1474	Not Resolved

Table 10: Identified Species in IM-MS Spectrum of 2-Hydroxypropyl-β-Cyclodextrin (Negative Mode)

2-Hydroxypropyl-Beta-Cyclodextrin: Negative Mode					
1- Charge State			2- Charge State		
Identity	Molecular Weight (g/mol)	Observed m/z	Identity	Molecular Weight (g/mol)	Observed m/z
M-H	1482.454	1481.7384	M-2H	1481.446	740.3687
M+Cl	1518.914	1517.7024	2M-2H	2964.907	1481.7374
2M-H	2965.915	2964.5605	2M+Na-3H	2986.889	1492.7272
			2M+K-3H	3002.997	1500.7245
			3M-2H	4448.368	2223.1162
			3M+Na-3H	4470.350	2234.0925
			3M+K-3H	4486.459	2242.0735
			4M-2H	5931.830	2964.5369

Table 11: Dependence of CCS ($Å^2$) on Wave Height

Wave Height (v)	[Leu-Enk+H]$^{1+}$	[SO+H]$^{1+}$	[SO+αCD+H]$^{1+}$	[SA+H]$^{1+}$	[SA+αCD+H]$^{1+}$	[PMG+H]$^{1+}$	[PMG+αCD+H+K]$^{2+}$	[Chol-H_2O+H]$^{1+*}$
25	126	134	223	136	225	212	221	136
30	109	135	210	137	212	212	190	134
35	94	142	200	144	203	218	153	134
40	69	143	187	146	188	225	98	104
Average	3	6	5	6	6	6	8	5
Standard Deviation	24	5	15	5	15	6	53	15
40V CCS/ 25V CCS	0.55	1.07	0.84	1.08	0.84	1.06	0.44	0.77

All data acquired on 7/25/11 except where noted

*Data Acquired on 4/13/12, T-Wave calibration redone on this date

REFERENCES

1. (a) Hempel, C. FDA Approves Request for New Cyclodextrin Treatment for Niemann Pick Type C. http://addiandcassi.com/fda-approves-request-cyclodextrin-treatment-niemann-pick-type/ (accessed June 13); (b) Davidson, C. D.; Ali, N. F.; Micsenyi, M. C.; Stephney, G.; Renault, S.; Dobrenis, K.; Ory, D. S.; Vanier, M. T.; Walkley, S. U., Chronic Cyclodextrin Treatment of Murine Niemann-Pick C Disease Ameliorates Neuronal Cholesterol and Glycosphingolipid Storage and Disease Progression. *PLoS ONE* **2009,** *4* (9), e6951.
2. Patterson, M. Niemann-Pick Disease Type C. . http://www.ncbi.nlm.nih.gov/books/NBK1296/ (accessed Mar 28).
3. Singh, I.; Kishimoto, Y., Effect of cyclodextrins on the solubilization of lignoceric acid, ceramide, and cerebroside, and on the enzymatic reactions involving these compounds. *Journal of Lipid Research* **1983,** *24* (5), 662-5.
4. Gimpl, G.; Gehrig-Burger, K., Probes for studying cholesterol binding and cell biology. *Steroids* **2011,** *76* (3), 216-231.
5. Loftsson, T.; Brewster, M. E., Pharmaceutical applications of cyclodextrins: basic science and product development. *J. Pharm. Pharmacol.* **2010,** *62* (Copyright (C) 2011 American Chemical Society (ACS). All Rights Reserved.), 1607-1621.
6. (a) Kralj, B.; Smidovnik, A.; Kobe, J., Mass spectrometric investigations of alpha- and beta-cyclodextrin complexes with ortho-, meta- and para-coumaric acids by negative mode electrospray ionization. *Rapid Commun Mass Spectrom* **2009,** *23* (1), 171-80; (b) Cescutti, P.; Garozzo, D.; Rizzo, R., Study of the inclusion complexes of aromatic molecules with cyclodextrins using ionspray mass spectrometry. *Carbohydrate Research* **1996,** *290* (2), 105-115; (c) Gabelica, V.; Galic, N.; De Pauw, E., On the specificity of cyclodextrin complexes detected by electrospray mass spectrometry. *J. Am. Soc. Mass Spectrom.* **2002,** *13* (8), 946-953; (d) Srinivasan, K.; Bartlett, M. G., Comparison of cyclodextrin-barbiturate noncovalent complexes using electrospray ionization mass spectrometry and capillary electrophoresis. *Rapid Communications in Mass Spectrometry* **2000,** *14* (8), 624-632.
7. (a) Ravichandran, R.; Divakar, S., Inclusion of Ring A of Cholesterol Inside the Œ≤-Cyclodextrin Cavity: Evidence from Oxidation Reactions and Structural Studies. *Journal of Inclusion Phenomena and Macrocyclic Chemistry* **1998,** *30* (3), 253-270; (b) Mohamed, M. H.; Wilson, L. D.; Headley, J. V.; Peru, K. M., Electrospray ionization mass spectrometry studies of cyclodextrin-carboxylate ion inclusion complexes. *Rapid Commun Mass Spectrom* **2009,** *23* (23), 3703-12.
8. Tabushi, I.; Kiyosuke, Y.; Sugimoto, T.; Yamamura, K., Approach to the aspects of driving force of inclusion by .alpha.-cyclodextrin. *Journal of the American Chemical Society* **1978,** *100* (3), 916-919.
9. (a) McDaniel, E. W.; Martin, D. W.; Barnes, W. S., Drift Tube-Mass Spectrometer for Studies of Low-Energy Ion-Molecule Reactions. *Rev. Sci. Instrum.* **1962,** *33* (1), 2; (b) Kanu, A. B.; Dwivedi, P.; Tam, M.; Matz, L.; Hill, H. H., Ion mobility–mass spectrometry. *Journal of Mass Spectrometry* **2008,** *43* (1), 1-22.
10. (a) Scarff, C. A.; Thalassinos, K.; Hilton, G. R.; Scrivens, J. H., Travelling wave ion mobility mass spectrometry studies of protein structure: biological significance and

comparison with X-ray crystallography and nuclear magnetic resonance spectroscopy measurements. *Rapid Communications in Mass Spectrometry* **2008,** *22* (20), 3297-3304; (b) Shvartsburg, A. A.; Smith, R. D., Fundamentals of Traveling Wave Ion Mobility Spectrometry. *Analytical Chemistry* **2008,** *80* (24), 9689-9699.
11. (a) Hilderbrand, A. E.; Myung, S.; Clemmer, D. E., Exploring Crown Ethers as Shift Reagents for Ion Mobility Spectrometry. *Analytical Chemistry* **2006,** *78* (19), 6792-6800; (b) Howdle, M.; Eckers, C.; Laures, A.; Creaser, C., The use of shift reagents in ion mobility-mass spectrometry: Studies on the complexation of an active pharmaceutical ingredient with polyethylene glycol excipients. *J. Am. Soc. Mass Spectrom.* **2009,** *20* (1), 1-9; (c) Bohrer, B. C.; Clemmer, D. E., Shift Reagents for Multidimensional Ion Mobility Spectrometry-Mass Spectrometry Analysis of Complex Peptide Mixtures: Evaluation of 18-Crown-6 Ether Complexes. *Analytical Chemistry* **2011,** *83* (13), 5377-5385.
12. Merenbloom, S. I.; Bohrer, B. C.; Koeniger, S. L.; Clemmer, D. E., Assessing the Peak Capacity of IMS-IMS
Separations of Tryptic Peptide Ions in He at 300 K. *Analytical Chemistry* **2006,** *79* (2), 515-522.
13. Giles, K.; Pringle, S. D.; Worthington, K. R.; Little, D.; Wildgoose, J. L.; Bateman, R. H., Applications of a travelling wave-based radio-frequency-only stacked ring ion guide. *Rapid Communications in Mass Spectrometry* **2004,** *18* (20), 2401-2414.
14. (a) Ruotolo, B. T.; Benesch, J. L. P.; Sandercock, A. M.; Hyung, S.-J.; Robinson, C. V., Ion mobility-mass spectrometry analysis of large protein complexes. *Nat. Protocols* **2008,** *3* (7), 1139-1152; (b) Bush, M. F.; Hall, Z.; Giles, K.; Hoyes, J.; Robinson, C. V.; Ruotolo, B. T., Collision Cross Sections of Proteins and Their Complexes: A Calibration Framework and Database for Gas-Phase Structural Biology. *Analytical Chemistry* **2010,** *82* (22), 9557-9565.
15. Waters SYNAPT G2 High Definition Mass Spectrometry System: Operator's Overview and Maintenance Guide. Waters Corporation: Wythenshawe, 2009.
16. Clemmer, D., Cross Section Database. 26 Oct 2006 ed.; Indiana University: 2006.
17. Short, L. C.; Syage, J. A., Electrospray photoionization (ESPI) liquid chromatography/mass spectrometry for the simultaneous analysis of cyclodextrin and pharmaceuticals and their binding interactions. *Rapid Communications in Mass Spectrometry* **2008,** *22* (4), 541-548.
18. Shvartsburg, A. A.; Bryskiewicz, T.; Purves, R. W.; Tang, K.; Guevremont, R.; Smith, R. D., Field Asymmetric Waveform Ion Mobility Spectrometry Studies of Proteins:‚Äâ Dipole Alignment in Ion Mobility Spectrometry? *The Journal of Physical Chemistry B* **2006,** *110* (43), 21966-21980.
19. (a) Polfer, N. C.; Bohrer, B. C.; Plasencia, M. D.; Paizs, B.; Clemmer, D. E., On the Dynamics of Fragment Isomerization in Collision-Induced Dissociation of Peptides. *The Journal of Physical Chemistry A* **2008,** *112* (6), 1286-1293; (b) Sztáray, J.; Memboeuf, A.; Drahos, L.; Vékey, K., Leucine enkephalin—A mass spectrometry standard. *Mass Spectrom Rev* **2011,** *30* (2), 298-320; (c) Schnier, P. D.; Jurchen, J. C.; Williams, E. R., The Effective Temperature of Peptide Ions Dissociated by Sustained Off-Resonance Irradiation Collisional Activation in Fourier Transform Mass Spectrometry. *The Journal of Physical Chemistry B* **1999,** *103* (4), 737-745; (d) Yamamoto, A.; Akanuma, S.-i.; Tachikawa, M.; Hosoya, K.-i., Involvement of LAT1 and LAT2 in the high- and low-affinity transport of L-leucine in human retinal pigment

epithelial cells (ARPE-19 cells). *J Pharm Sci* **2010,** *99* (5), 2475-2482; (e) Pak, A.; Lesage, D.; Gimbert, Y.; Vékey, K.; Tabet, J.-C., Internal energy distribution of peptides in electrospray ionization : ESI and collision-induced dissociation spectra calculation. *Journal of Mass Spectrometry* **2008,** *43* (4), 447-455.